white adipose tissues of 8-week-old ARKO males. As no significant alterations in food intake were observed, our results suggested that AR may serve as a negative regulator of adipocyte development in adult males (Fig. 4C).

Drosophila model to dissect human AR mutants with expanded polyQ stretches in neurodegeneration

Another characteristic clinical disorder with an AR mutation is spinal and bulbar muscular atrophy (SBMA), also known as Kennedy's disease (*5*, *7*). SBMA is a rare degenerative disease of the motor neurons characterized by progressive muscle atrophy and weakness in male patients, usually beginning at 30 to 50 years of age. Previous analyses of SBMA revealed expansions in the number of trinucleotide CAG repeats in the first exon of the AR gene, which generated expanded polyQ stretches in the A/B domain of the AR protein (*5*, *7*, *20*). It was found that disease onset occurred when these repeat stretches encoded more than 40 glutamine residues, compared to a range of 15 to 35 polyQ residues in normal individuals.

To dissect the molecular mechanism of human AR (hAR) mutants with expanded polyQ stretches in neurodegeneration, we established a *Drosophila* model that ectopically overexpressed a mutated AR in photoreceptor neurons (*13*). We first expressed WT and mutated hAR in photoreceptor neurons in developing eye discs under the glass multimer reporter (*GMR*) gene promoter (*21*) using the *Drosophila melanogaster* GAL4-UAS system (*22*). To monitor the ligand-induced transactivation function of hAR, hAR-expressing flies were further crossed to flies carrying a *GFP* reporter gene, with the result that GFP expression was induced by the binding of ligand-bound AR to the consensus *ARE* in the GFP promoter (*23*). Expressed hAR proteins were then detected as red fluorescence *in situ* using an immunofluorescent antibody.

Although eyes that expressed a mutant hAR containing an expanded 52-stretch polyQ (Q52) appeared normal, dietary ingestion of dihydrotestosterone (DHT) or androgen antagonists induced marked degeneration and apoptosis of the photoreceptor neurons, despite the mutant hAR retaining only reduced transactivation function. Ligand-independent toxicity was detected in fly eyes expressing truncated polyQ-expanded A/B domains alone, but this was abrogated by the co-expression of unliganded LBD domains. Thus, our results suggested that hormone binding and subsequent structural alteration of hAR mutants with nuclear localization appeared to be critical for SBMA onset (Fig. 5), and that the fly-eye model may be useful for the development of novel therapeutic approaches to SBMA.

We thank members of the laboratory of Nuclear Signaling, IMCB for support and H. Higuchi for manuscript preparation. This work was supported in part by a grant-in-aid for priority areas from the Ministry of Education, Science, Sports and Culture of Japan (K.-i.T. and S.K.).

REFERENCES

1. Mooradian, A.D., Morley, J.E., and Korenman, S.G. (1987) Biological actions of androgens. *Endocr. Rev.* **8**, 1–28
2. Wilson, J.D. (1999) The role of androgens in male gender role behavior. *Endocr. Rev.* **20**, 726–737
3. Glass, C.K. and Rosenfeld, M.G. (2000) The coregulator exchange in transcriptional functions of nuclear receptors. *Genes Dev.* **14**, 121–141
4. Mangelsdorf, D.J., Thummel, C., Beato, M., Herrlich, P., Schutz, G., Umesono, K., Blumberg , B., Kastner, P., Mark, M., Chambon, P., and *et al.* (1995) The nuclear receptor superfamily: the second decade. *Cell* **83**, 835–839
5. Choong, C.S. and Wilson, E.M. (1998) Trinucleotide repeats in the human androgen receptor: a molecular basis for disease. *J. Mol. Endocrinol.* **21**, 235–257
6. Griffin, J.E. (1992) Androgen resistance–the clinical and molecular spectrum. *N. Engl. J. Med.* **326**, 611–618
7. La Spada, A.R., Wilson, E.M., Lubahn, D.B., Harding, A.E., and Fischbeck, K.H. (1991) Androgen receptor gene mutations in X-linked spinal and bulbar muscular atrophy. *Nature* **352**, 77–79
8. McPhaul, M.J. (1999) Molecular defects of the androgen receptor. *J. Steroid Biochem. Mol. Biol.* **69**, 315–322
9. Quigley, C.A., De Bellis, A., Marschke, K.B., el-Awady, M.K., Wilson, E.M., and French, F.S. (1995) Androgen receptor defects: historical, clinical, and molecular perspectives. *Endocr. Rev.* **16**, 271–321
10. Sato, T., Matsumoto, T., Yamada, T., Watanabe, T., Kawano, H., and Kato, S. (2003) Late onset of obesity in male androgen receptor-deficient (AR KO) mice. *Biochem. Biophys. Res. Commun.* **300**, 167–171
11. Sato, T., Matsumoto, T., Kawano, H., Watanabe, T., Uematsu, Y., Sekine, K., Fukuda, T., Aihara, K., Krust, A., Yamada, T., Nakamichi, Y., Yamamoto, Y., Nakamura, T., Yoshimura, K., Yoshizawa, T., Metzger, D., Chambon, P., and Kato, S. (2004) Brain masculinization requires androgen receptor function. *Proc. Natl Acad. Sci. USA* **101**, 1673–1678
12. Kawano, H., Sato, T., Yamada, T., Matsumoto, T., Sekine, K., Watanabe, T., Nakamura, T., Fukuda, T., Yoshimura, K., Yoshizawa, T., Aihara, K., Yamamoto, Y., Nakamichi, Y., Metzger, D., Chambon, P., Nakamura, K., Kawaguchi, H., and Kato, S. (2003) Suppressive function of androgen receptor in bone resorption. *Proc. Natl Acad. Sci. USA* **100**, 9416–9421
13. Takeyama, K., Ito, S., Yamamoto, A., Tanimoto, H., Furutani, T., Kanuka, H., Miura, M., Tabata, T., and Kato, S. (2002) Androgen-dependent neurodegeneration by polyglutamine-expanded human androgen receptor in Drosophila. *Neuron* **35**, 855–864
14. Lubahn, D.B., Joseph, D.R., Sullivan, P.M., Willard, H.F., French, F.S., and Wilson, E.M. (1988) Cloning of human androgen receptor complementary DNA and localization to the X chromosome. *Science* **240**, 327–330
15. Poujol, N., Wurtz, J.M., Tahiri, B., Lumbroso, S., Nicolas, J.C., Moras, D., and Sultan, C. (2000) Specific recognition of androgens by their nuclear receptor. A structure-function study. *J. Biol. Chem.* **275**, 24022–24031
16. Shiau, A.K., Barstad, D., Loria, P.M., Cheng, L., Kushner, P.J., Agard, D.A., and Greene, G.L. (1998) The structural basis of estrogen receptor/coactivator recognition and the antagonism of this interaction by tamoxifen. *Cell* **95**, 927–937
17. Yanagisawa, J., Kitagawa, H., Yanagida, M., Wada, O., Ogawa, S., Nakagomi, M., Oishi, H., Yamamoto, Y., Nagasawa, H., McMahon, S.B., Cole, M.D., Tora, L., Takahashi, N., and Kato, S. (2002) Nuclear receptor function requires a TFTC-type histone acetyl transferase complex. *Mol. Cell* **9**, 553–562
18. Kato, S., Endoh, H., Masuhiro, Y., Kitamoto, T., Uchiyama, S., Sasaki, H., Masushige, S., Gotoh, Y., Nishida, E., Kawashima, H., and *et al.* (1995) Activation of the estrogen receptor through phosphorylation by mitogen-activated protein kinase. *Science* **270**, 1491–1494
19. Li, M., Indra, A.K., Warot, X., Brocard, J., Messaddeq, N., Kato, S., Metzger, D., and Chambon, P. (2000) Skin abnormalities generated by temporally controlled RXRalpha mutations in mouse epidermis. *Nature* **407**, 633–636

20. Merry, D.E., Kobayashi, Y., Bailey, C.K., Taye, A.A., and Fischbeck, K.H. (1998) Cleavage, aggregation and toxicity of the expanded androgen receptor in spinal and bulbar muscular atrophy. *Hum. Mol. Genet.* **7**, 693–701
21. Moses, K. and Rubin, G.M. (1991) Glass encodes a site-specific DNA-binding protein that is regulated in response to positional signals in the developing Drosophila eye. *Genes Dev.* **5**, 583–593
22. Brand, A.H. and Perrimon, N. (1993) Targeted gene expression as a means of altering cell fates and generating dominant phenotypes. *Development* **118**, 401–415
23. Yamamoto, A., Hashimoto, Y., Kohri, K., Ogata, E., Kato, S., Ikeda, K., and Nakanishi, M. (2000) Cyclin E as a coactivator of the androgen receptor. *J. Cell Biol.* **150**, 873–880.

Premature ovarian failure in androgen receptor-deficient mice

Hiroko Shiina*†‡, Takahiro Matsumoto*‡§, Takashi Sato*, Katsuhide Igarashi¶, Junko Miyamoto*, Sayuri Takemasa*, Matomo Sakari*§, Ichiro Takada*, Takashi Nakamura*§, Daniel Metzger‖, Pierre Chambon‖, Jun Kanno¶, Hiroyuki Yoshikawa†, and Shigeaki Kato*§**

*Institute of Molecular and Cellular Biosciences, University of Tokyo, 1-1-1 Yayoi, Bunkyo-ku, Tokyo 113-0032, Japan; §Exploratory Research for Advanced Technology, Japan Science and Technology, 4-1-8 Honcho, Kawaguchi, Saitama 332-0012, Japan; †Department of Obstetrics and Gynecology, Institute of Clinical Medicine, University of Tsukuba, 1-1-1 Tennoudai, Tsukuba, Ibaraki 305-8575, Japan; ¶Division of Cellular and Molecular Toxicology, National Institute of Health Sciences, 1-18-1 Kamiyoga, Setagaya-ku, Tokyo 158-8501, Japan; and ‖Institut de Genetique et de Biologie Moleculaire et Cellulaire, Centre National de la Recherche Scientifique, Institut National de la Santé et de la Recherche Médicale, Universite Louis Pasteur, College de France, 67404 Illkirch, Strasbourg, France

Edited by Bert W. O'Malley, Baylor College of Medicine, Houston, TX, and approved November 10, 2005 (received for review August 5, 2005)

Premature ovarian failure (POF) syndrome, an early decline of ovarian function in women, is frequently associated with X chromosome abnormalities ranging from various Xq deletions to complete loss of one of the X chromosomes. However, the genetic locus responsible for the POF remains unknown, and no candidate gene has been identified. Using the Cre/LoxP system, we have disrupted the mouse X chromosome androgen receptor (*Ar*) gene. Female $AR^{-/-}$ mice appeared normal but developed the POF phenotype with aberrant ovarian gene expression. Eight-week-old female $AR^{-/-}$ mice are fertile, but they have lower follicle numbers and impaired mammary development, and they produce only half of the normal number of pups per litter. Forty-week-old $AR^{-/-}$ mice are infertile because of complete loss of follicles. Genome-wide microarray analysis of mRNA from $AR^{-/-}$ ovaries revealed that a number of major regulators of folliculogenesis were under transcriptional control by AR. Our findings suggest that AR function is required for normal female reproduction, particularly folliculogenesis, and that AR is a potential therapeutic target in POF syndrome.

male hormone | nuclear receptor | female physiology | folliculogenesis | kit ligand

Premature ovarian failure (POF) is defined as an early decline of ovarian function after seemingly normal folliculogenesis (1). Genetic causes of POF have been frequently associated with X chromosome abnormalities (1, 2). Complete loss of one of the X chromosomes, as in Turner syndrome, and various Xq deletions are commonly identified as a cause of POF. However, responsible X-linked genes and their downstream targets have not been identified so far.

The androgen receptor (*Ar*) gene, which is the only sex hormone receptor gene on the X chromosome, is well known to be essential not only for the male reproductive system, but also for male physiology. In contrast, androgens are considered as male hormones; therefore, little is known about androgens' actions in female physiology, although AR expression in growing follicles has been described (3). However, because excessive androgen production in polycystic ovary syndrome causes infertility with abnormal menstrual cycles (4, 5), it is possible that AR-mediated androgen signaling also plays an important physiological role in the female reproductive system. Recently, using Cre/LoxP system, we generated an AR-null mutant mouse line (6) and demonstrated that inactivation of AR resulted in arrest of testicular development and spermatogenesis, impaired brain masculinization, high-turnover osteopenia, and late onset of obesity in males (7–9). At the same time, no overt physical or growth abnormalities were observed in female $AR^{-/-}$ mice. Therefore, to further examine potential role of AR in female physiology, we characterized female reproductive system in $AR^{-/-}$ females. Herein we show that female $AR^{-/-}$ mice develop the POF phenotype. At 3 weeks of age, $AR^{-/-}$ females had apparently normal ovaries with numbers of follicles similar to those in the wild-type females. However, thereafter the number of healthy follicles in the $AR^{-/-}$ ovary gradually declined, with a marked increase of atretic follicles, and by 40 weeks $AR^{-/-}$ mice became infertile, with no follicle detectable in the ovary. Reflecting this age-dependent progression in ovarian abnormality, several genes known to be involved in the oocyte–granulosa cell regulatory loop were identified by microarray analysis as AR downstream target genes. These findings clearly demonstrate that AR-mediated androgen signaling is indispensable for the maintenance of folliculogenesis and implicate impaired androgen signaling as a potential cause of the POF syndrome.

Materials and Methods

Generation of AR Knockout Mice. *AR* genomic clones were isolated from a TT2 embryonic stem cell genomic library by using human *AR* A/B domain cDNA as a probe (6). The targeting vector consisted of a 7.6-kb 5′ region containing exon 1, a 1.3-kb 3′ homologous region, a single loxP site, and a neo cassette with two loxP sites (10). Targeted clones (FB-18 and FC-61) were aggregated with single eight-cell embryos from CD-1 mice (11, 12). Floxed *AR* mice (C57BL/6) were then crossed with CMV-Cre transgenic mice (6). The two lines exhibited the same phenotypic abnormalities. The chromosomal sex of each pup was determined by genomic PCR amplification of the Y chromosome *Sry* gene (13).

Western Blot Analysis. To detect AR protein expression, ovarian cell lysates were separated by SDS/PAGE and transferred onto nitrocellulose membranes (14). Membranes were probed with polyclonal AR antibodies (N-20; Santa Cruz Biotechnology), and blots were visualized by using peroxidase-conjugated second antibody and an ECL detection kit (Amersham Pharmacia Biosciences).

Morphologic Classification of Growing Follicles. Sections were taken at intervals of 30 μm, and 6-μm paraffin-embedded sections were mounted on slides. Routine hematoxylin and eosin staining was performed for histologic examination by light microscopy. Follicle numbers in 12 sections per ovary were evaluated as primary follicles (oocyte surrounded by a single layer of cuboidal granulosa cells), preantral follicles (oocyte surrounded by two or

Conflict of interest statement: No conflicts declared.

This paper was submitted directly (Track II) to the PNAS office.

Abbreviations: AR, androgen receptor; DHT, 5α-dihydrotestosterone; POF, premature ovarian failure.

‡H.S. and T.M. contributed equally to this work.

**To whom correspondence should be addressed. E-mail: uskato@mail.ecc.u-tokyo.ac.jp.

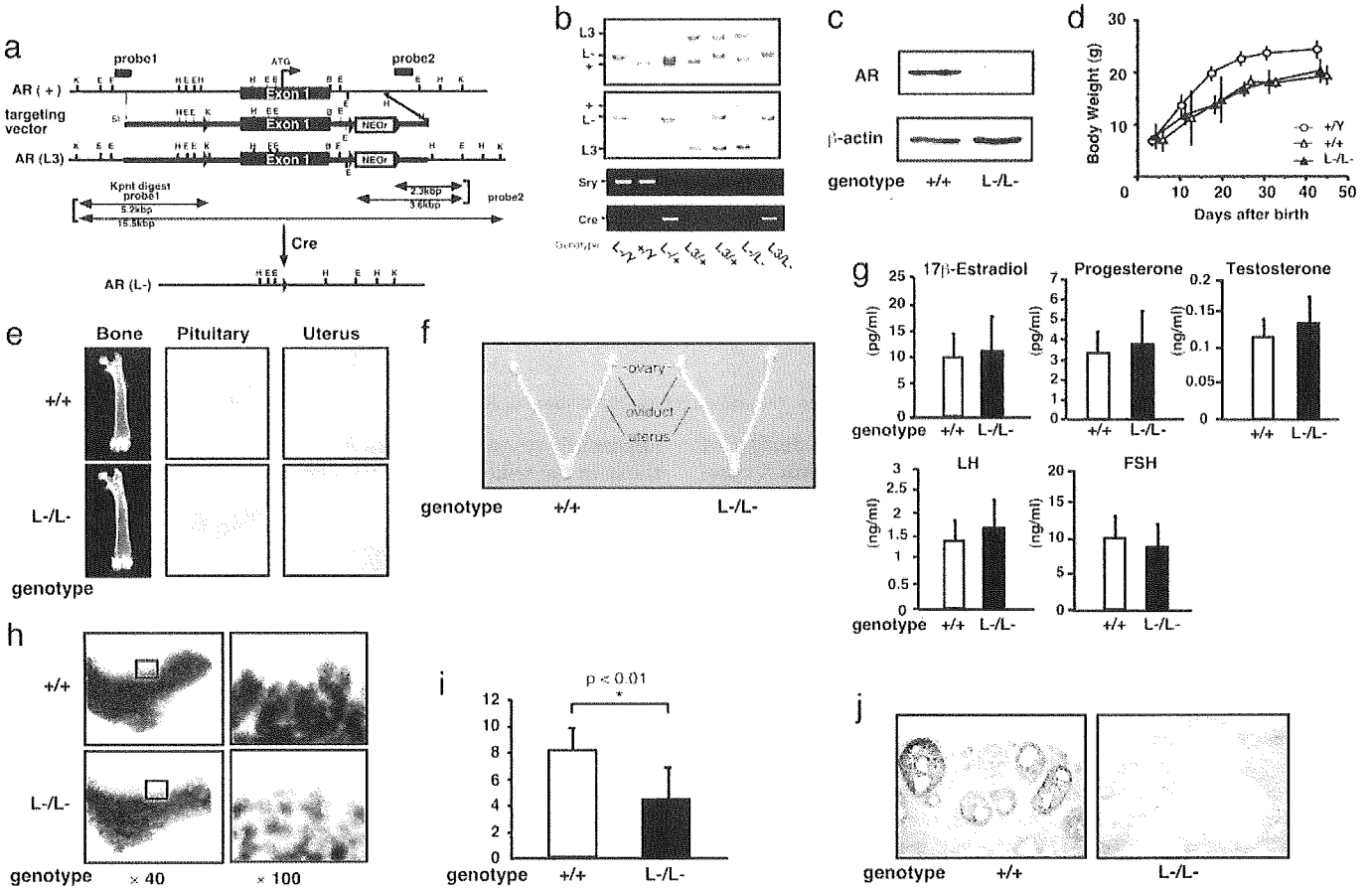

Fig. 1. Phenotypic characterization of AR knockout female mice. (*a*) Diagram of the wild-type *Ar* genomic locus (+), floxed *AR* L3 allele (L3), and *AR* allele (L-) obtained after Cre-mediated excision of exon 1. K, KpnI; E, EcoRI; H, HindIII; B, BamHI. LoxP sites are indicated by arrowheads. The targeting vector consisted of a 7.6-kb 5′ homologous region containing exon 1, a 1.3-kb 3′ homologous region, a single loxP site, and the neo cassette with two loxP sites. (*b*) Detection of the Y chromosome-specific *Sry* gene in $AR^{-/Y}$ mice by PCR. (*c*) Absence of AR protein in $AR^{-/-}$ mice ovaries by Western blot analysis using a specific C-terminal antibody. (*d*) Normal weight gain in $AR^{-/-}$ females. (*e*) Histology of pituitary, uterus, and bone tissues in $AR^{+/+}$ and $AR^{-/-}$ females at 8 weeks of age. (*f*) Female reproductive organs were macroscopically normal in $AR^{-/-}$ mice. (*g*) Serum hormone levels at the proestrus stage in $AR^{-/-}$ mice were not significantly altered. Serum 17β-estradiol, progesterone, testosterone, luteinizing hormone (LH), and follicle-stimulating hormone (FSH) levels in $AR^{+/+}$ ($n = 13$) and $AR^{-/-}$ ($n = 10$) females at 8–10 weeks of age are shown. (*h*) Lobuloalveolar development is impaired in $AR^{-/-}$ mammary glands. Whole mount of inguinal mammary glands (*Left*) and its higher magnification (*Right*) were prepared on day 3 of lactation. (*i*) Average number of pups per litter is markedly reduced in $AR^{-/-}$ mice at 8 weeks of age. Data are shown as mean ± SEM and analyzed by using Student's *t* test. (*j*) AR immunocytochemistry in $AR^{+/+}$ and $AR^{-/-}$ ovaries. Sections were counterstained with eosin.

more layers of granulosa cells with no antrum), or antral follicles (antrum within the granulosa cell layers enclosing the oocyte). Follicles were determined to be atretic if they displayed two or more of the following criteria within a single cross section: more than two pyknotic nuclei, granulosa cells within the antral cavity, granulosa cells pulling away from the basement membrane, or uneven granulosa cell layers (15).

Immunohistochemistry. Sections were subjected to a microwave antigen retrieval technique by boiling in 10 mM citrate buffer (pH 6.0) in a microwave oven for 30 min (16). The cooled sections were incubated in 1% H_2O_2 for 30 min to quench endogenous peroxidase and then incubated with 1% Triton X-100 in PBS for 10 min. To block nonspecific antibody binding, sections were incubated in normal goat serum for 1 h at 4°C. Sections were then incubated with anti-AR (1:100) or anti-cleaved caspase-3 (1:100) in 3% BSA overnight at 4°C. Negative controls were incubated in 3% BSA without primary antibody. The ABC method was used to visualize signals according to the manufacturer's instructions. Sections were incubated in biotinylated goat anti-rabbit IgG (1:200 dilution) for 2 h at room temperature, washed with PBS, and incubated in avidin–biotin–horseradish peroxidase for 1 h. After thorough washing in PBS, sections were developed with 3,3′-diaminobendizine tetrahydrochloride substrate, slightly counterstained with eosin, dehydrated through an ethanol series and xylene, and mounted.

Estrus Cycles and Fertility Test. To determine the stage of the estrus cycle (proestrus, estrus, and diestrus), vaginal smears were taken every morning and stained with Giemsa solution. For evaluation of female fertility for 15 weeks, an 8- or 24-week-old wild-type or $AR^{-/-}$ female was mated with a wild-type fertile male, replaced every 2 weeks with the other fertile male. Cages were monitored daily and for an additional 23 days, and the presence of seminal plugs and number of litters were recorded.

RNA Extraction and Quantitative Competitive RT-PCR. Total ovarian RNA was extracted by using TRIzol (Invitrogen) (16). Oligo-dT-primed cDNA was synthesized from 1 μg of ovarian RNA by using SuperScript reverse transcriptase (Gibco BRL, Gaithersburg, MD) in a 20-μl reaction volume, 1 μl of which was then diluted serially (2- to 128-fold) and used to PCR-amplify an internal control gene, *cycA*, to allow concentration estimation.

PHYSIOLOGY

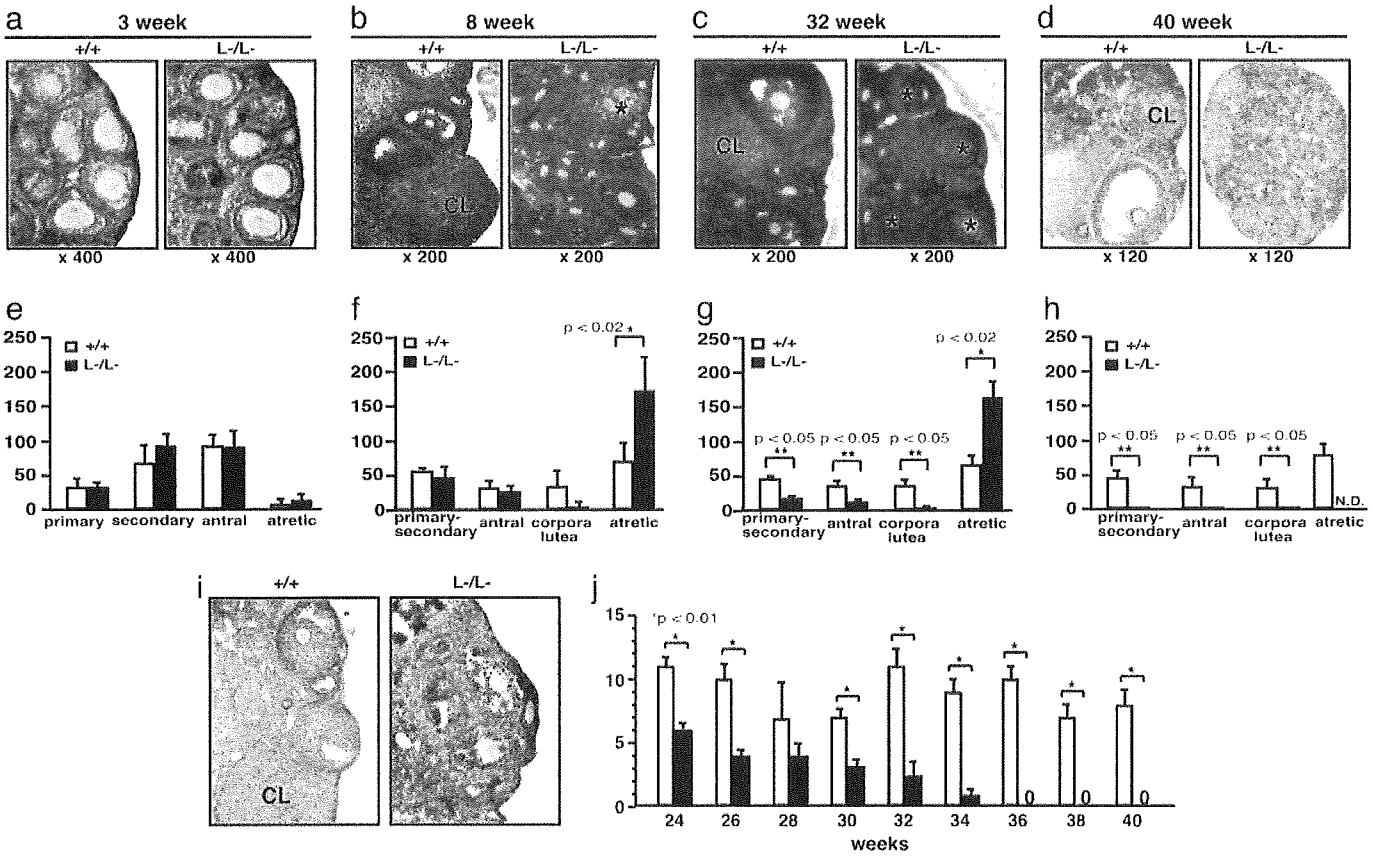

Fig. 2. POF in $AR^{-/-}$ female mice. (*a–d*) Histology of $AR^{+/+}$ and $AR^{-/-}$ ovaries at 3 weeks, 8 weeks, 32 weeks, and 40 weeks of age. All sections were stained with hematoxylin and eosin. An asterisk marks the atretic follicle. CL, corpus luteum. (*e–h*) Relative follicle counts at 3 weeks (*e*), 8 weeks (*f*), 32 weeks (*g*), and 40 weeks (*h*) of age. Numbers represent total counts of every fifth section from serially sectioned ovaries ($n = 4$ animals per genotype). (*i*) Immunohistochemical study for activated, cleaved caspase-3 revealed increased positive cells (apoptotic cells) in $AR^{-/-}$ ovaries. Sections were counterstained with hematoxylin. An asterisk marks the caspase-3-positive cell. CL, corpus luteum. (*j*) Age-dependent reduction in the number of pups per litter in $AR^{-/-}$ female mice. A continuous breeding assay was started at 24 weeks of age ($n = 6–10$ animals per genotype). For all panels, data are shown as mean ± SEM and were analyzed by using Student's *t* test.

Primers were designed from cDNA sequences of *Kitl* (M57647; nucleotides 1099–1751), Gdf9 (NM008110; nucleotides 720-1532), *Bmp15* (NM009757; nucleotides 146–973), *Ers2* (NM010157; nucleotides 1139–1921), *Pgr* (NM008829; nucleotides 1587–2425), *Cyp11a1* (NM019779; nucleotides 761-1697), *Cyp17al* (M64863; nucleotides 522–932), *Cyp19* (D00659; nucleotides 699-1049), *Fshr* (AF095642; nucleotides 625-1427), *Lhr* (M81310; nucleotides 592-1331), *Ptgs2* (AF338730; nucleotides 3–605), and *Ccnd2* (NM009829; nucleotides 150-1065) and chosen from different exons to avoid amplification from genomic DNA.

GeneChip Analysis. Ovaries were isolated and stabilized in RNA*later* RNA Stabilization Reagent (Ambion, Austin, TX) before RNA purification (17). Total RNA was purified by using an RNeasy mini kit (Qiagen, Valencia, CA) according to the manufacturer's instructions. First-strand cDNA was synthesized from 5 μg of RNA by using 200 units of SuperScript II reverse transcriptase (Invitrogen, Carlsbad, CA), 100 pmol T7-$(dT)_{24}$ primer [5′-GGCCAGTGAATTGTAATACGACTCAC-TATAGGGAGGCGG-$(dT)_{24}$-3′], 1× first-strand buffer, and 0.5 mM dNTPs at 42°C for 1 h. Second-strand synthesis was performed by incubating first-strand cDNA with 10 units of *Escherichia coli* ligase (Invitrogen), 40 units of DNA polymerase I (Invitrogen), 2 units of RNase H (Invitrogen), 1× reaction buffer, and 0.2 mM dNTPs at 16°C for 2 h, followed by 10 units of T4 DNA polymerase (Invitrogen) and incubation for another 5 min at 16°C. Double-stranded cDNA was purified by using GeneChip Sample Cleanup Module (Affymetrix, Santa Clara, CA) according to the manufacturer's instructions and labeled by *in vitro* transcription by using a BioArray HighYield RNA transcript labeling kit (Enzo Diagnostics, Farmingdale, NY). Briefly, dsDNA was mixed with 1× HY reaction buffer, 1× biotin-labeled ribonucleotides (NTPs with Bio-UTP and Bio-CTP), 1× DTT, 1× RNase inhibitor mix, and 1× T7 RNA polymerase and incubated at 37°C for 4 h. Labeled cRNA was then purified by using GeneChip Sample Cleanup Module and fragmented in 1× fragmentation buffer at 94°C for 35 min. For hybridization to the GeneChip Mouse Expression Array 430A or 430B or Mouse Genome 430 2.0 Array (Affymetrix), 15 μg of fragmented cRNA probe was incubated with 50 pM control oligonucleotide B2, 1× eukaryotic hybridization control, 0.1 mg/ml herring sperm DNA, 0.5 mg/ml acetylated BSA, and 1× hybridization buffer in a 45°C rotisserie oven for 16 h. Washing and staining were performed by using a GeneChip Fluidic Station (Affymetrix) according to the manufacturer's protocol. Phycoerythrin-stained arrays were scanned as digital image files and analyzed with GENECHIP OPERATING SOFTWARE (Affymetrix) (17).

Luciferase Assay. The *Kitl* promoter region (−2866 to −1 bp) was inserted into the pGL3-basic vector (Promega) for assay using the Luciferase Assay System (Promega) (14, 16). Cells at 40–50% confluence were transfected with a reference pRL-CMV

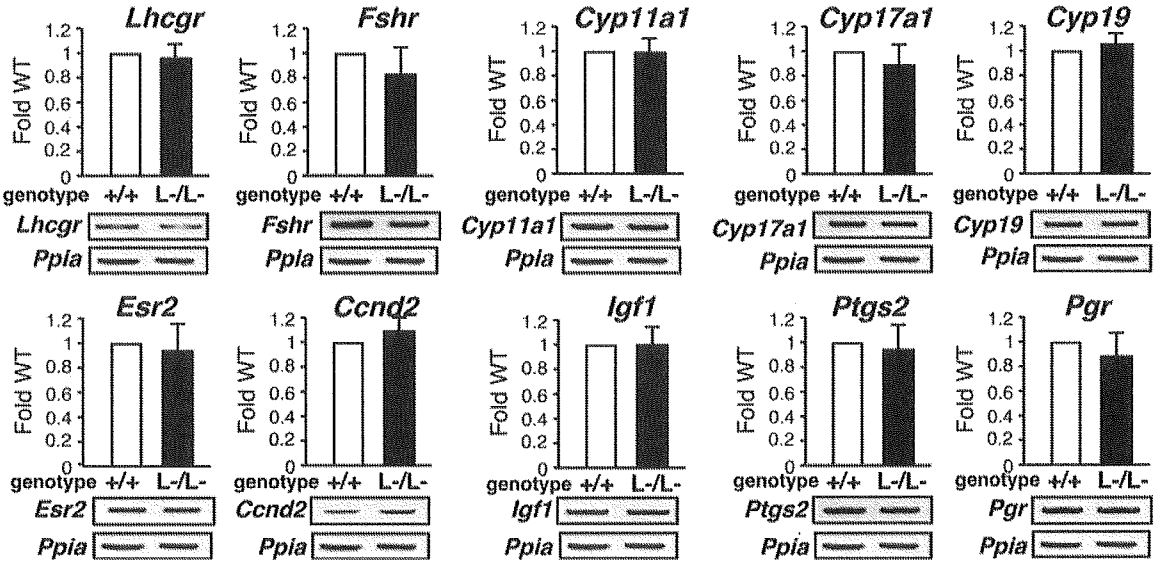

Fig. 3. No significant alterations in mRNA levels of several major regulators in folliculogenesis. Shown is semiquantitative RT-PCR of LH receptor (*Lhr*), FSH receptor (*Fshr*), p450 side chain cleavage enzyme (*Cyp11a1*), 17-α-hydroxylase (*Cyp17a1*), Aromatase (*Cyp19*), estrogen receptor-β (*Esr2*), cyclin D2 (*Ccnd2*), insulin-like growth factor 1 (*Igf1*), cyclooxygenase 2 (*Ptgs2*), or progesterone receptor (*Pgr*) gene expression in $AR^{+/+}$ and $AR^{-/-}$ ovaries. Results shown were representative (using one ovary per genotype in each experiment) of five independent experiments.

plasmid (Promega) using Lipofectamine reagent (GIBCO/BRL, Grand Island, NY) to normalize transfection. Results shown are representative of five independent experiments.

Results and Discussion

Subfertility of $AR^{-/-}$ Female Mice at 8 Weeks of Age. The *Ar* gene located on the X chromosome was disrupted in mice by using the Cre/Lox P system (6) (Fig. 1 *a–c*). Female $AR^{-/-}$ mice showed normal growth compared with the wild-type littermates (Fig. 1*d*), with no detectable bone loss (Fig. 1*e*) or obesity common for male $AR^{-/Y}$ mice (8, 9). Young (8-week-old) $AR^{-/-}$ females appeared indistinguishable from the wild-type littermates, displayed normal sexual behavior (7), and produced the first offspring of normal body size at the expected age. Macroscopic appearance of their reproductive organs, including uteri, oviducts, and ovaries, also appeared normal (Fig. 1*f*). Histological analysis showed no significant abnormality in the uterus or pituitary (Fig. 1*e*), whereas mammary ductal branching and elongation were substantially reduced, as revealed by whole-mount analysis (Fig. 1*h*). Serum levels of 17β-estradiol, progesterone, testosterone, luteinizing hormone, and follicle-stimulating hormone were also within normal range in 8-week-old mutant females at the proestrus stage (Fig. 1*g*), suggesting that the two-cell two-gonadotrophin system in female reproductive and endocrine organs (18) was intact in $AR^{-/-}$ mice at 8 weeks of age. The most obvious early sign of abnormal reproductive function in the $AR^{-/-}$ females was that their average numbers of pups per litter were only about half of those of the wild-type littermates, ($AR^{+/+}$, 8.3 ± 0.4 pups per litter; $AR^{-/-}$, 4.5 ± 0.5 pups per litter) (Fig. 1*i*).

$AR^{-/-}$ Female Mice Developed POF Phenotypes. Histological analysis of 8-week-old $AR^{-/-}$ ovaries clearly showed that numbers of atretic follicles were significantly increased, with decreased numbers of corpora lutea (Fig. 2 *b* and *f*). This finding suggests that the reduced pup numbers were due to impaired folliculogenesis in AR-deficient ovaries. Indeed, AR protein expression was readily detectable in the wild-type 8-week-old ovaries (Fig. 1*j*), with AR expressed at the highest levels in growing follicle granulosa cells at all developmental stages and at relatively low levels in corpora lutea. Thus, AR appears to play a regulatory role in granulosa cells during their maturation to the luteal phase.

To investigate this possibility, we examined the ovarian phenotype of female $AR^{-/-}$ mice at different ages. At 3 weeks, ovaries contain various stages of follicles, including primary, secondary, and antral follicles in wild-type animals (Fig. 2*a*) (19). In $AR^{-/-}$ ovaries at 3 weeks of age, the folliculogenesis appeared to be unaltered, with normal numbers and localization of primary and secondary follicles (Fig. 2 *a* and *e*). However, degenerated folliculogenesis became evident with further aging. Although follicles and corpora lutea at all developmental stages were still present, corpora lutea numbers were clearly reduced in 8-week-old $AR^{-/-}$ mutants (Fig. 2 *b* and *f*), similar to that observed in another mouse line (20). Expected apoptosis was seen in atretic follicles by activated caspase-3 immunohistochemistry assays (Fig. 2*i*). But, by 32 weeks of age, defects in folliculogenesis in $AR^{-/-}$ ovaries became profound, with fewer follicles observed and increased atretic follicles (Fig. 2 *c* and *g*), and >40% (5 of 12 mice) of the $AR^{-/-}$ females were already infertile. By 40 weeks, all $AR^{-/-}$ females became infertile, with no follicles remaining (Fig. 2 *d* and *h*); at the same age, $AR^{+/+}$ females were fertile and had normal follicle numbers. Consistent with progressive deficiency in folliculogenesis, the pup number per litter steadily decreased in aging $AR^{-/-}$ females (Fig. 2*i*). These data indicate that AR plays an important physiological role at the preluteal phase of folliculogenesis.

Alteration in Gene Expressions of Several Major Regulators Involved in the Oocyte–Granulosa Cell Regulatory Loop. To explore the molecular basis underlying the impaired folliculogenesis in $AR^{-/-}$ ovaries, we analyzed expression of several major known regulators and markers of folliculogenesis (21–23). Surprisingly, no significant alterations in mRNA levels of LH receptor (*Lhr*), FSH receptor (*Fshr*), p450 side chain cleavage enzyme (*Cyp11a1*), 17-α-hydroxylase (*Cyp17a1*), aromatase (*Cyp19*), estrogen receptor-β (*Esr2*), cyclin D2 (*Ccnd2*), or insulin-like growth factor 1 (*Igf1*) of 8-week-old $AR^{-/-}$ ovaries at the proestrus stage, and further cyclooxygenase 2 (*Ptgs2*) or progesterone receptor (*Pgr*) at the estrus stage, were detected by

PHYSIOLOGY

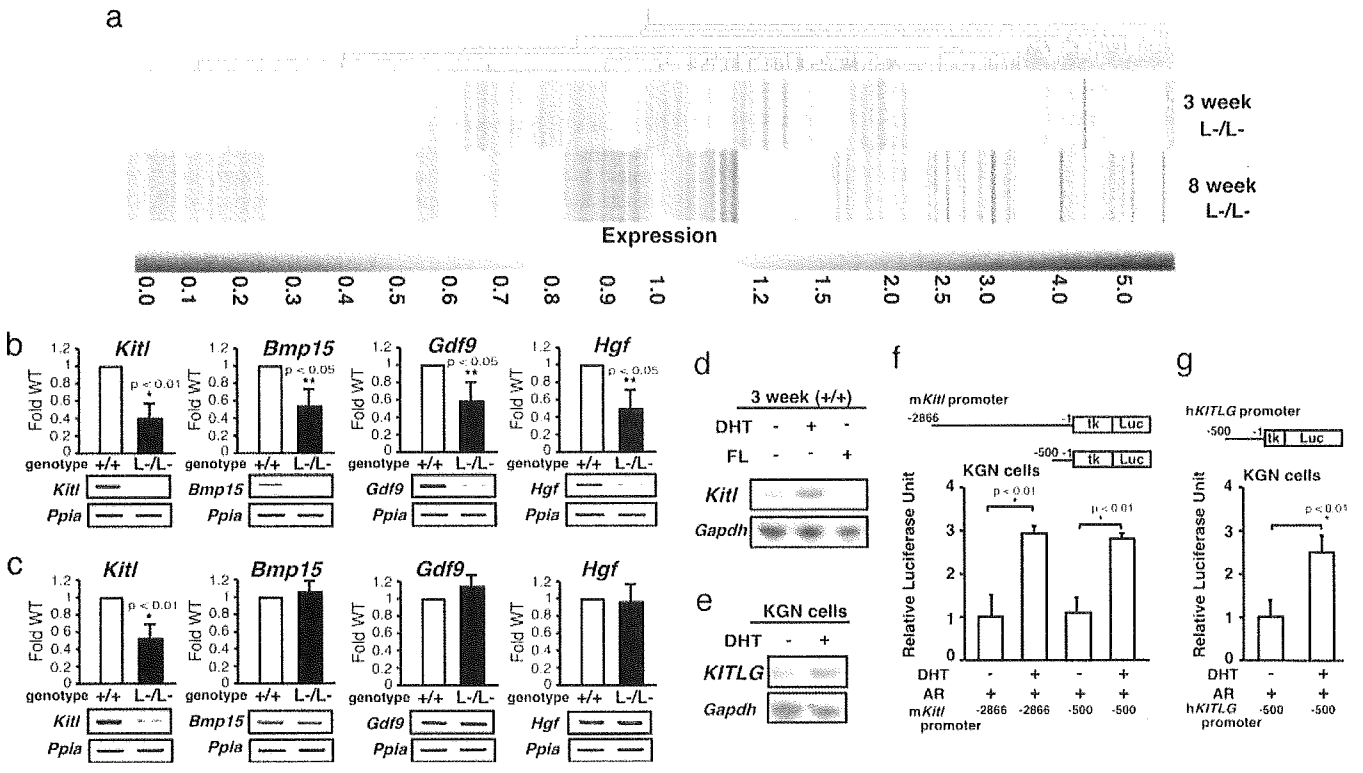

Fig. 4. Genome-wide microarray analysis and semiquantitative RT-PCR revealed that expression of the oocyte–granulosa cell regulator loop was down-regulated in $AR^{-/-}$ ovaries. (*a*) Microarray analysis of $AR^{-/-}$ compared with $AR^{+/+}$ ovaries at 3 and 8 weeks of age. Data obtained from microarray analysis as described in *Materials and Methods* were used to generate a cluster analysis. Each vertical line represents a single gene. The ratios of gene expression levels in $AR^{-/-}$ ovaries compared with wild type are presented. (*b* and *c*) Semiquantitative RT-PCR analysis of AR-regulated genes identified from the microarray study. Results shown are representative (using one ovary per genotype in each experiment) of five independent experiments. Data are shown as mean ± SEM and were analyzed by using Student's *t* test. (*d*) Comparison of *Kitl* gene expression by Northern blot analysis among placebo-, DHT-, and flutamide (FL)-treated $AR^{+/+}$ mouse ovaries. (e) Induction of *KITLG* gene expression by DHT treatment in KGN cells. (*f* and *g*) Androgen responsiveness in the mouse and human *kit ligand* promoters by a luciferase assay performed by using KGN cells. Data are shown as mean ± SEM and were analyzed by using Student's *t* test.

semiquantitative RT-PCR analysis (Fig. 3). Genome-wide microarray analysis (17) of RNA from 8-week-old $AR^{-/-}$ ovaries at the proestrus stage has been undertaken to identify AR-regulated genes. In comparison with $AR^{+/+}$ ovaries, expressions of 772 genes were down-regulated, whereas 351 genes were up-regulated in $AR^{-/-}$ ovaries (Fig. 4*a*; see also Tables 1 and 2, which are published as supporting information on the PNAS web site). Several genes known to be involved in the oocyte–granulosa cell regulatory loop (24) were identified as candidate AR target genes, including KIT ligand (*Kitl*) (25), morphogenetic protein 15 (*Bmp15*) (26), growth differentiation factor-9 (*Gdf9*) (27), and hepatocyte growth factor (*Hgf*) (28). Impaired folliculogenesis had been reported in mice deficient in each of these three regulators (26, 27, 29). To validate the microarray data, we performed semiquantitative RT-PCR analysis of 8-week-old $AR^{-/-}$ ovary RNA and confirmed that expression of these factors was down-regulated (Fig. 4*b*). To identify a regulator downstream of the AR signaling at an earlier stage of folliculogenesis, 3-week-old $AR^{-/-}$ ovaries that, as pointed out earlier, display no apparent phenotypic abnormality were examined. Fewer genes had altered expression levels (519 genes up-regulated; 326 genes down-regulated) (Fig. 4*a*; see also Tables 3 and 4, which are published as supporting information on the PNAS web site), and, of the four regulators tested by RT-PCR, only *Kitl* was found to be down-regulated at this age (Fig. 4*c*). Because *Kitl* is a granulosa cell-derived factor and stimulates oocyte growth and maturation (29–31), down-regulation of the *Kitl* expression in 3-week-old or even younger $AR^{-/-}$ ovaries may trigger impairment in folliculogenesis at a later age. To test for possible *Kitl* gene regulation by AR, 3-week-old wild-type females were treated with 5α-dihydrotestosterone (DHT). At 4 h after hormone injection, a clear induction of *Kitl* expression was observed in the ovaries, whereas a known antiandrogen flutamide attenuated the induction by DHT (Fig. 4*d*). The induction of endogenous human *kit ligand* (*KITLG*) gene by DHT was also observed in human granulosa-like tumor cells (KGN) in culture (Fig. 4*e*). Furthermore, androgen-induced transactivation of mouse and human *kit ligand* promoters (32) was observed by a luciferase reporter assay (33) in KGN (Fig. 4 *f* and *g*), 293T, and HeLa (data not shown) cells. However, no response to DHT was detected in the similar assay using promoters of the *Bmp15*, *Gdf9*, and *Hgf* genes (data not shown). Thus, we have shown that, in a regulatory cascade controlling folliculogenesis, *Kitl* represents a direct downstream target of androgen signaling.

As an upstream regulator, AR may also be indirectly involved in control of expression of other genes critical for folliculogenesis, because an age-dependent down-regulation of *Bmp15*, *Gdf9*, and *Hgf* gene expression was also observed in $AR^{-/-}$ ovaries. *Bmp15* and *Gdf9* are oocyte-derived factors that promote the development of surrounding granulosa cells in growing follicles (34, 35), whereas *Hgf* is secreted by theca cells and acts as a granulosa cell growth factor (36). Down-regulation of these factors, presumably due to decreased *Kitl* expression, may lead to impaired bidirectional communication between oocyte and granulosa cells (24) and, eventually, to early termination of folliculogenesis, as in POF syndrome.

Thus, we have identified AR as a novel regulator of follicu-

logenesis that apparently acts in the regulatory cascade upstream of the major factors controlling ovarian function, confirming the previous findings of the AR expression in granulose cells of growing follicles (3). Although not immediately relevant to the ovarian physiology, abnormal development of the mammary glands observed in our AR-deficient mice adds further strong evidence of an essential role of the AR not only in male, but also in female, reproductive function.

With increasing age of the first childbirth by women in the modern society, POF syndrome has become an important social and medical problem. Our findings suggest that POF syndrome may be caused by an impairment in androgen signaling and that X chromosomal mutations affecting the *AR* gene function may play a key role in hereditary POF. From clinical perspective, the present study provides evidence that AR can be a beneficial therapeutic target in treatment of POF syndrome patients.

We thank T. Iwamori and H. Tojo for expert advice on mammary gland anatomy, Y. Kanai for ovarian phenotypic analysis, members of the KO project team at the laboratory of Nuclear Signaling (Institute of Molecular and Cellular Biosciences) for their support, A. P. Kouzmenko for helpful suggestions, and H. Higuchi for manuscript preparation. This work was supported in part by the Program for Promotion of Basic Research Activities for Innovative Biosciences and priority areas from the Ministry of Education, Culture, Sports, Science, and Technology (to S.K.).

1. Laml, T., Preyer, O., Umek, W., Hengstschlager, M. & Hanzal, H. (2002) *Hum. Reprod. Update* **8,** 483–491.
2. Davison, R. M., Davis, C. J. & Conway, G. S. (1999) *Clin. Endocrinol. (Oxford)* **51,** 673–679.
3. Tetsuka, M., Whitelaw, P. F., Bremner, W. J., Millar, M. R., Smyth, C. D. & Hillier, S. G. (1995) *J. Endocrinol.* **145,** 535–543.
4. Ehrmann, D. A., Barnes, R. B. & Rosenfield, R. L. (1995) *Endocr. Rev.* **16,** 322–353.
5. Norman, R. J. (2002) *Mol. Cell. Endocrinol.* **191,** 113–119.
6. Kato, S. (2002) *Clin. Pediatr. Endocrinol.* **11,** 1–7.
7. Sato, T., Matsumoto, T., Kawano, H., Watanabe, T., Uematsu, Y., Sekine, K., Fukuda, T., Aihara, K., Krust, A., Yamada, T., *et al.* (2004) *Proc. Natl. Acad. Sci. USA* **101,** 1673–1678.
8. Sato, T., Matsumoto, T., Yamada, T., Watanabe, T., Kawano, H. & Kato, S. (2003) *Biochem. Biophys. Res. Commun.* **300,** 167–171.
9. Kawano, H., Sato, T., Yamada, T., Matsumoto, T., Sekine, K., Watanabe, T., Nakamura, T., Fukuda, T., Yoshimura, K., Yoshizawa, T., *et al.* (2003) *Proc. Natl. Acad. Sci. USA* **100,** 9416–9421.
10. Li, M., Indra, A. K., Warot, X., Brocard, J., Messaddeq, N., Kato, S., Metzger, D. & Chambon, P. (2000) *Nature* **407,** 633–636.
11. Sekine, K., Ohuchi, H., Fujiwara, M., Yamasaki, M., Yoshizawa, T., Sato, T., Yagishita, N., Matsui, D., Koga, Y., Itoh, N. & Kato, S. (1999) *Nat. Genet.* **21,** 138–141.
12. Yoshizawa, T., Handa, Y., Uematsu, Y., Takeda, S., Sekine, K., Yoshihara, Y., Kawakami, T., Arioka, K., Sato, H., Uchiyama, Y., *et al.* (1997) *Nat. Genet.* **16,** 391–396.
13. Gubbay, J., Collignon, J., Koopman, P., Capel, B., Economou, A., Munsterberg, A., Vivian, N., Goodfellow, P. & Lovell-Badge, R. (1990) *Nature* **346,** 245–250.
14. Yanagisawa, J., Yanagi, Y., Masuhiro, Y., Suzawa, M., Watanabe, M., Kashiwagi, K., Toriyabe, T., Kawabata, M., Miyazono, K. & Kato, S. (1999) *Science* **283,** 1317–1321.
15. Britt, K. L., Drummond, A. E., Cox, V. A., Dyson, M., Wreford, N. G., Jones, M. E., Simpson, E. R. & Findlay, J. K. (2000) *Endocrinology* **141,** 2614–2623.
16. Ohtake, F., Takeyama, K., Matsumoto, T., Kitagawa, H., Yamamoto, Y., Nohara, K., Tohyama, C., Krust, A., Mimura, J., Chambon, P., *et al.* (2003) *Nature* **423,** 545–550.
17. Fujimoto, N., Igarashi, K., Kanno, J., Honda, H. & Inoue, T. (2004) *J. Steroid Biochem. Mol. Biol.* **91,** 121–129.
18. Couse, J. F. & Korach, K. S. (1999) *Endocr. Rev.* **20,** 358–417.
19. Elvin, J. A. & Matzuk, M. M. (1998) *Rev. Reprod.* **3,** 183–195.
20. Hu, Y. C., Wang, P. H., Yeh, S., Wang, R. S., Xie, C., Xu, Q., Zhou, X., Chao, H. T., Tsai, M. Y. & Chang, C. (2004) *Proc. Natl. Acad. Sci. USA* **101,** 11209–11214.
21. Elvin, J. A., Yan, C., Wang, P., Nishimori, K. & Matzuk, M. M. (1999) *Mol. Endocrinol.* **13,** 1018–1034.
22. Zhou, J., Kumar, T. R., Matzuk, M. M. & Bondy, C. (1997) *Mol. Endocrinol.* **11,** 1924–1933.
23. Burns, K. H., Yan, C., Kumar, T. R. & Matzuk, M. M. (2001) *Endocrinology* **142,** 2742–2751.
24. Matzuk, M. M., Burns, K. H., Viveiros, M. M. & Eppig, J. J. (2002) *Science* **296,** 2178–2180.
25. Joyce, I. M., Pendola, F. L., Wigglesworth, K. & Eppig, J. J. (1999) *Dev. Biol.* **214,** 342–353.
26. Yan, C., Wang, P., DeMayo, J., DeMayo, F. J., Elvin, J. A., Carino, C., Prasad, S. V., Skinner, S. S., Dunbar, B. S., Dube, J. L., *et al.* (2001) *Mol. Endocrinol.* **15,** 854–866.
27. Dong, J., Albertini, D. F., Nishimori, K., Kumar, T. R., Lu, N. & Matzuk, M. M. (1996) *Nature* **383,** 531–535.
28. Parrott, J. A., Vigne, J. L., Chu, B. Z. & Skinner, M. K. (1994) *Endocrinology* **135,** 569–575.
29. Driancourt, M. A., Reynaud, K., Cortvrindt, R. & Smitz, J. (2000) *Rev. Reprod.* **5,** 143–152.
30. Huang, E. J., Manova, K., Packer, A. I., Sanchez, S., Bachvarova, R. F. & Besmer, P. (1993) *Dev. Biol.* **157,** 100–109.
31. Packer, A. I., Hsu, Y. C., Besmer, P. & Bachvarova, R. F. (1994) *Dev. Biol.* **161,** 194–205.
32. Grimaldi, P., Capolunghi, F., Geremia, R. & Rossi, P. (2003) *Biol. Reprod.* **69,** 1979–1988.
33. Kitagawa, H., Fujiki, R., Yoshimura, K., Mezaki, Y., Uematsu, Y., Matsui, D., Ogawa, S., Unno, K., Okubo, M., Tokita, A., *et al.* (2003) *Cell* **113,** 905–917.
34. Otsuka, F. & Shimasaki, S. (2002) *Proc. Natl. Acad. Sci. USA* **99,** 8060–8065.
35. Joyce, I. M., Clark, A. T., Pendola, F. L. & Eppig, J. J. (2000) *Biol. Reprod.* **63,** 1669–1675.
36. Parrott, J. A. & Skinner, M. K. (1998) *Endocrinology* **139,** 2240–2245.

Oncogene (2005) 24, 3206–3215

www.nature.com/onc

Domain-specific function of ShcC docking protein in neuroblastoma cells

Izumi Miyake[1,2], Yuko Hakomori[1], Yoko Misu[2], Hisaya Nakadate[2], Nobuo Matsuura[2], Michiie Sakamoto[3] and Ryuichi Sakai*[,1]

[1]*Growth Factor Division, National Cancer Center Research Institute, 5-1-1 Tsukiji, Chuo-ku, Tokyo 104-0045, Japan;* [2]*Department of Pediatrics, Kitasato University School of Medicine, 1-15-1 Kitasato, Sagamihara-shi, Kanagawa 228-8555, Japan;* [3]*Department of Pathology, Keio University School of Medicine, 35 Shinanomachi, Shinjuku-ku, Tokyo 160-8582, Japan*

ShcC is a family member of the Shc docking proteins that possess two different phosphotyrosine-binding motifs and conduct signals as Grb2-binding substrates of various receptor tyrosine kinases. We have recently shown that some neuroblastoma cell lines, such as NB-39-nu cells, express a protein complex of hyperphosphorylated ShcC and anaplastic lymphoma kinase (ALK), which is self-activated by gene amplification. Here, we demonstrate that the expression of a mutant ShcC lacking Grb2-binding sites, 3YF-ShcC, significantly impaired the survival, differentiation and motility of NB-39-nu cells by blocking the ERK and Akt pathways. On the other hand, cells overexpressing ShcC or 3YF-ShcC, but not a mutant ShcC that lacks SH2, showed decreased anchorage independency and *in vivo* tumorigenicity, suggesting a novel ShcC-specific suppressive effect through its SH2 domain on cell transformation. Notably, overexpression of ShcC suppressed the sustained phosphorylation of Src family kinase after cell detachment, which might be independent of phosphorylation of Grb2-binding site. It was indicated that the Src/Fyn-Cas pathway is modulated as a target of these suppressive effects by ShcC. Reciprocal change of ShcC expression and phosphorylation observed in malignant neuroblastoma cell lines might be explained by these phosphotyrosine-dependent and -independent functions of ShcC.
Oncogene (2005) **24,** 3206–3215. doi:10.1038/sj.onc.1208523
Published online 21 February 2005

Keywords: ShcC; neuroblastoma; dominant-negative form; SH2 domain; Src family kinase

Introduction

The Shc family of docking proteins plays an essential role in leading cellular signaling to specific downstream molecules such as the Ras-ERK pathway and the phosphatidylinositol 3-kinase (PI3 K)-Akt pathway when recruited towards phosphotyrosine residues of various activated RTKs. In mammals, three *shc* genes have been identified, and their products have been termed ShcA/Shc, ShcB/Sli/Sck and ShcC/Rai/N-Shc (Nakamura *et al.*, 1996a; O'Bryan *et al.*, 1996b; Pelicci *et al.*, 1996). ShcA is ubiquitously expressed in most organs except the adult neural system, whereas ShcB and ShcC proteins are selectively expressed in the neural system within adult mouse tissues.

The Shc family molecules have a unique PTB-CH1-SH2 modular organization. Two phosphotyrosine-binding modules, PTB and SH2 domains, recognize phosphotyrosine-containing polypeptides such as cytoplasmic domains of various activated RTKs (Pelicci *et al.*, 1992; van der Geer *et al.*, 1995). The CH1 domain has several tyrosine phosphorylation sites that recruit other SH2-containing adaptor molecules such as Grb2 (van der Geer *et al.*, 1996; Thomas and Bradshaw, 1997) and a proline-rich stretch of ShcA composing the binding site for the SH3 domains of other proteins including Src, Fyn and Lyn (Weng *et al.*, 1994; Wary *et al.*, 1998). There might be difference in the molecular functions of each Shc family member, although there is not much information on individual roles of Shc families in the neural system and neuronal tumors.

We have recently shown that the expression and tyrosine phosphorylation of Shc family proteins, especially ShcC, are observed in most neuroblastoma cells. Stable association of constitutively activated anaplastic lymphoma kinase (ALK) with the ShcC has been observed in several neuroblastoma cell lines that have extremely high phosphorylation levels of ShcC (Miyake *et al.*, 2002). These cell lines showed malignant phenotypes as for tumorigenicity in nude mice or soft agar colony assay, and notably, ShcC expression is low compared with other neuroblastoma in spite of significantly high phosphorylation state. The *ALK* gene locus was significantly amplified in these cell lines, which results in the constitutive activation of the ALK and most prominent tyrosine phosphorylation of ShcC among several known binding partners of ALK such as PLCγ and IRS-1 (Miyake *et al.*, 2002).

ALK protein has the typical structure of an RTK classified into the insulin receptor superfamily. It is dominantly expressed in the normal neural system (Iwahara *et al.*, 1997; Morris *et al.*, 1997), although the biological role of this protein in neuronal cells has not yet been clearly identified. We detected remarkable amplification of the *ALK* gene in three out of 13 neuroblastoma cell lines (Miyake *et al.*, 2002) and a less

*Correspondence: R Sakai; E-mail: rsakai@gan2.res.ncc.go.jp
Received 12 October 2004; revised 30 December 2004; accepted 12 January 2005; published online 21 February 2005

significant gain of copy numbers in eight out of 85 primary neuroblastoma tissues (Hakomori *et al.*, manuscript in preparation), most of which accompany the amplification of the *N-myc* gene. The three *ALK*-amplified neuroblastoma cell lines showed constitutive activation of full-length ALK and the increased local concentration of receptor tyrosine kinases appeared to interfere with signals from other RTKs. It is possible that ALK-ShcC signal activation has additional effects on the malignant tumor progression of neuroblastoma, probably similar to the mechanism reported in EGFR and Neu/ErbB2 (Andrechek *et al.*, 2000; Pawson *et al.*, 2001).

To clarify the role of hyperphosphorylated ShcC in neuroblastoma cells, the 3YF-ShcC mutant, which has phenylalanines at three Grb2-binding tyrosines (Y221/222/304) of ShcC, was utilized in this study in the expectation of a dominant-negative effect specific for signals originating from the ShcC-Grb2 complex. The biological effects of the 3YF-ShcC mutant as well as wild-type ShcC and the ΔSH2 ShcC mutant, which lacks the SH2 domain, were analysed to elucidate both Grb2-dependent and -independent functions of ShcC in neuroblastoma.

Results

Suppression of ERK1/2 and Akt activation in NB-39-nu cells by expression of 3YF-ShcC

A neuroblastoma cell line, NB-39-nu, was used in this study because it shows high tumorigenicity and anchorage independency with prominent phosphorylation level of ShcC caused by constitutively activated ALK kinase. The expression level of ShcC is relatively low among the neuroblastoma cell lines examined in our previous study. T7-tagged ShcC constructs containing the full length of human ShcC cDNA (ShcC-wt), a tyrosine-to-phenylalanin mutant for all three putative Grb2-binding sites (3YF-ShcC), and the SH2-deletion mutant (ΔSH2-ShcC) were subcloned into a mammalian expression vector, pcDNA3.1. Multiple independent clones of NB-39-nu cell lines stably expressing these ShcC mutants at comparable levels were selected and submitted to biochemical and biological analysis. Results of representative clones are shown in Figure 1a, although basically same results were obtained from other independent clones (data not shown). Tyrosine phosphorylation of the 3YF-ShcC was significantly suppressed suggesting that the three tyrosines lost in this mutant are the main phosphorylation sites of ShcC in NB-39-nu (Figure 1a). As expected, the complex formation of 3YF-ShcC with Grb2 was impaired, regardless of EGF stimulation, compared with that of ShcC-wt and ΔSH2-ShcC (Figure 1c). The activation level of ERK1/2 at 5 min after the EGF stimulation was decreased by expression of 3YF-ShcC, while expression of ShcC-wt or ΔSH2-ShcC did not affect the levels of ERK1/2 activation compared with the control cells transfected only by expression vector (mock) (Figure 1d). The phosphorylation level of Akt at Ser-473 was also suppressed by expression of 3YF-ShcC, although not at a similar level as that of cells treated with Wortmannin (Sigma), a PI3K inhibitor (Figure 1e). These analyses were performed using at least two independent clones. It was confirmed that 3YF-ShcC-expression has a dominant-negative effect on the PI3K/Akt pathway as well as the Ras/ERK pathway in this neuroblastoma cell line.

Expression of 3YF-ShcC increased susceptibility to retinoic acid (RA)-induced apoptosis in NB-39-nu cells

There were no obvious differences in growth rate among the NB-39-nu clones expressing each ShcC mutant (Figure 2a), whereas the rate of [^{3}H]-thymidine incorporation of the cell lines expressing 3YF-ShcC was slightly lower than that of other cells (Figure 2b).

The cytological analyses of the cells cultured with 10 μM of all-*trans*-RA revealed that 3YF-ShcC expressing cells were more susceptible to RA-induced apoptosis than the control or ShcC-wt-expressing cells (Figure 3a). Treatment of NB-39-nu cells, especially ShcC-wt-expressing cells, with RA at a lower concentration of 2.5 or 5 μM induced mild neurite formation, flattened, substrate-adherent cells resembling epithelial cells within 48 h (Figure 3b), which is known to be a characteristics of RA-induced morphologic differentiation (Sidell *et al.*, 1983). In contrast, this type of differentiation was not observed in 3YF-ShcC-expressing cells. Along with the suppressive effects of 3YF-ShcC to the Akt pathway (Figure 1e), these results suggest that phosphorylated ShcC plays significant role in survival signals through the putative Grb2-binding sites in NB-39-nu cells.

ShcC plays a distinct role in the migration of ALK-ShcC-activated neuroblastoma cells

Expression of 3YF-ShcC significantly suppresses cell migration ability as shown by the wound-healing assay (Figure 4a). A modified Boyden chamber cell-migration assay without Matrigel using fibronectin as a chemoattractant showed the results consistent with those obtained in the wound-healing assay (Figure 4b). A similar assay with Matrigel coating on a chamber filter to evaluate the chemotactic invasive activity of each transfectant also showed decreased invasive activity in 3YF-ShcC-expressing cells (Figure 4c). In contrast, ShcC-wt expression increased the migration ability of NB-39-nu cells both in wound healing assay and modified Boyden chamber assay without Matrigel (Figure 4a, b), while the ΔSH2-ShcC expression presented no remarkable effects on the cell motility. The invasive activity of ShcC-wt-expressing cells was not significantly high compared to that of the control or of the ΔSH2-ShcC-expressing cells (Figure 4c).

Expression of ShcC-wt or 3YF-ShcC has a negative effect on the transforming activity of NB-39-nu cells

Cells expressing ShcC-wt or 3YF-ShcC tend to grow to confluence with a monolayer appearance, making a clear

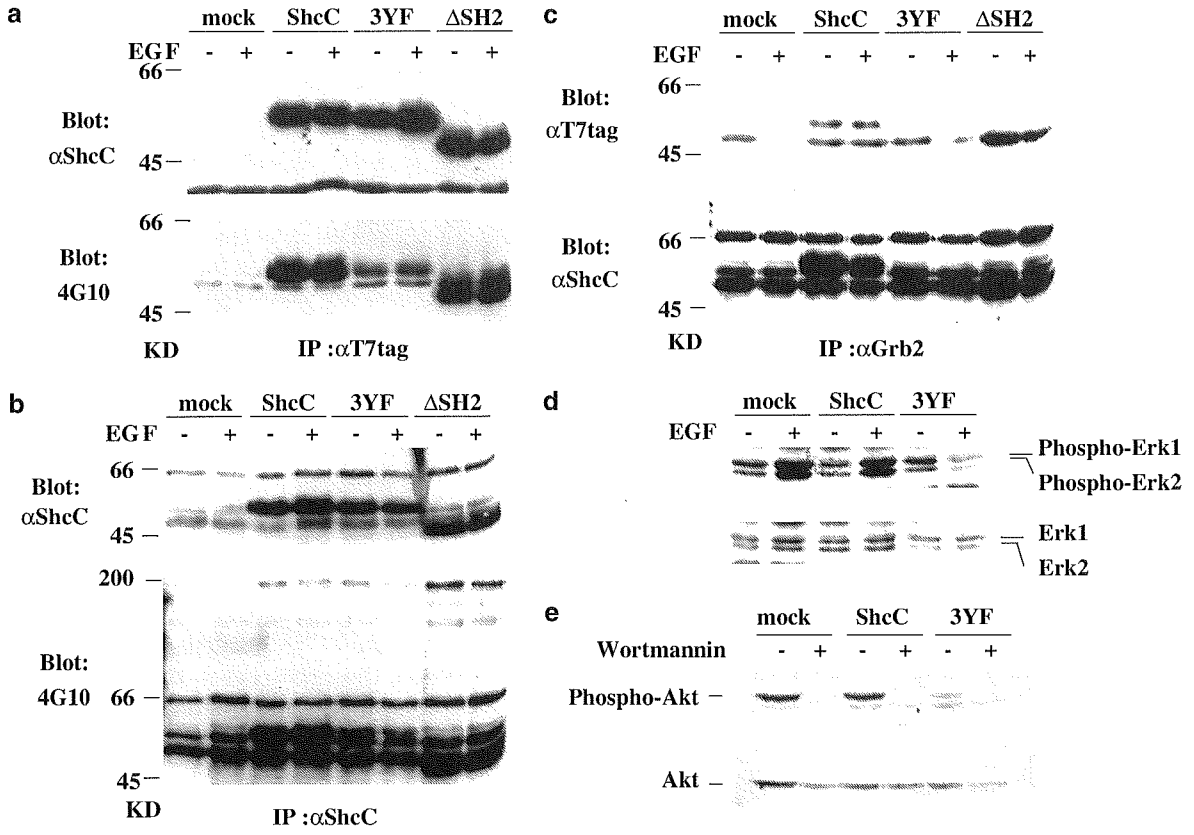

Figure 1 NB-39-nu cells stably expressing ShcC mutants analysed by immunoblotting. (**a**) Expression (upper panel) and tyrosine phosphorylation (lower panel) of ectopic ShcC mutant proteins (mock: control, ShcC: ShcC-wt, 3YF: 3YF-ShcC and ΔSH2: ΔSH2-ShcC) in the NB-39-nu cells. (**b**) Expression (upper panel) and tyrosine phosphorylation (lower panel) of both endogenous ShcC and ectopic ShcC mutants in NB-39-nu cells. (**c**) The complex formation of Grb2 with ShcC (lower panel) or ectopic ShcC mutants (upper panel) was analysed. (**d**) The activation of ERK1/2 in ShcC mutant cells. (**e**) Akt (Ser473) phosphorylation in ShcC mutant cells in a tissue culture medium with 10% fetal calf serum (FCS). For the negative control, the cells were treated with 1 μM of Wortmannin for 2 h. EGF stimulations were performed as described in Materials and methods. Lysates were duplicated and detected by the antibodies shown in the figure

difference from original NB-39-nu cells that tend to form cell aggregations on the culture dishes (Figure 5a). In addition, control NB-39-nu cells and ΔSH2-ShcC-expressing cells form a considerable number of colonies in soft agar (Figure 5b), which is significantly suppressed by the expression of ShcC-wt or 3YF-ShcC (Figure 5b). These results indicate that ShcC-wt or 3YF-ShcC have inhibitory effect on the transforming activity of NB-39-nu cells, especially anchorage-independent growth. Since the overexpression of ShcC had no significant effect on the activation of ERK1/2 or Akt in our experiment, it was suggested that a unique signaling pathway rather than classical Grb2-Ras pathway is involved in this phenomenon.

Src family kinases (SFKs) are well known to be associated with the ability to induce cellular transformation including anchorage independency (Parsons and Weber, 1989; Windham *et al*., 2002). During the investigation of ShcC mutant cells in the suspension state, we noticed that the sustained activation of both Fyn and c-Src observed in the control cells and ΔSH2-ShcC-expressing cells was suppressed by the expression of ShcC-wt or 3YF-ShcC (Figure 6a, b) at 24 h after cell detachment. Especially, the condition of phosphorylation of Fyn at suspension culture well correlated with anchorage independency of NB-39-nu sublines (Figure 6a). Tendency of phosphorylation of Src Tyr-416, which indicates the kinase activation of SFKs, is consistent with these results (Figure 6c). Phosphorylation of Cas, a main substrate of SFKs, in a suspended condition has recently been associated with the anchorage-independent growth of cancer-like lung adenocarcinoma (Wei *et al*., 2002). Sustention and temporary elevation of the Cas phosphorylation was also observed specifically in the original NB-39-nu cells, control and ΔSH2-ShcC-expressing cells, whereas there was a marked decrease of the phosphorylation level of Cas in ShcC-wt- and 3YF-ShcC-expressing cells (Figure 6d, e). Treatment of NB-39-nu control cells with PP2, a Src-specific inhibiter, suppressed the phosphorylation of Cas both in an attached and suspended condition, suggesting that the anchorage-independent phosphorylation of Cas is associated with the activity of the SFKs (Figure 6f).

The activation of ERK1/2 or Akt was similarly suppressed by suspension culture for 24 h regardless of the expression of each ShcC mutants although the basal

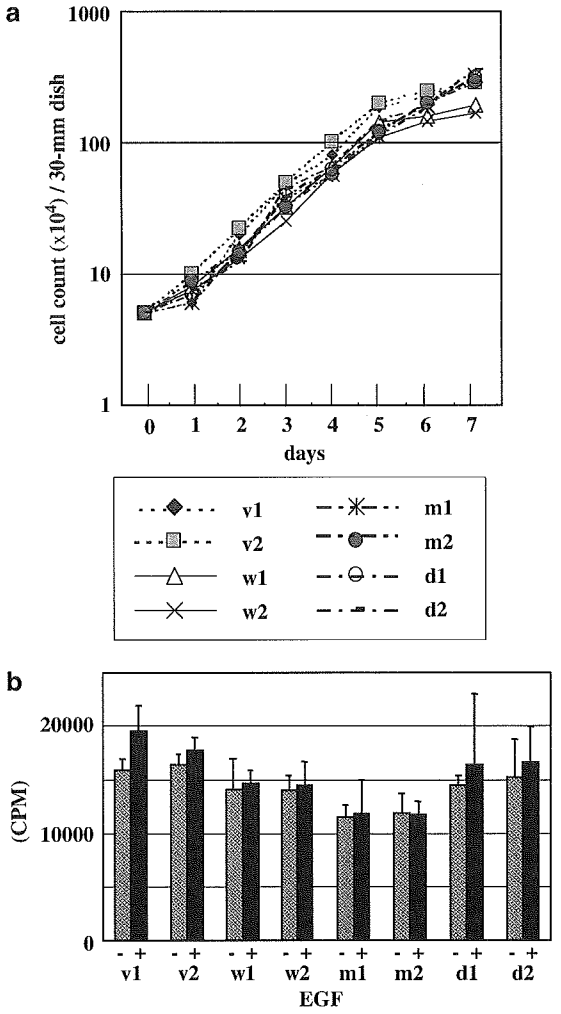

Figure 2 Growth rate and proliferation ability of ShcC mutant cells *in vitro*. (**a**) ShcC mutant cells cultured in a normal medium with 10% FCS by 30-mm dishes were counted at the indicated time points. The results represent the average values (±s.d.) of three replicated experiments for each clone. (**b**) ShcC mutant cells stimulated with none (gray bar) or EGF (black bar) were treated with [^{3}H]thymidine to the culture medium as described in Materials and methods. The graph represents the average values (±s.d.) from an experiment performed in triplicate. NB-39-nu clones are described as: v1 and v2 (control), w1 and w2 (expressing ShcC-wt), m1 and m2 (expressing 3YF), d1 and d2 (expressing ΔSH2)

level is lower in 3YF-ShcC clones (Supplementary Figure A). There were no difference in phosphorylation level of FAK and paxillin, which plays an important role in regulating the signals from the extracellular matrix (ECM) and organizing the actin-cytoskeleton, by expressing ShcC-wt, showing a similar level of decrease in the suspended condition (Supplementary Figure B). In summary, it was confirmed in this system that the constitutive activation of SFKs, such as Fyn and c-Src, and phosphorylation of Cas in suspended cells, but not other components of integrin signals such as FAK, is strictly linked to the anchorage independency of NB-39-nu cells, closely related with ShcC mutants expression. Furthermore, we detected interaction between ShcC-wt and some of SFKs following the stimulation (Figure 6g), indicating a novel biological interaction of ShcC with SFK, as suggested for ShcA in integrin pathway (Wary *et al*., 1996; Giancotti, 1997)

Loss of tumorigenicity of NB-39-nu-expressing ShcC-wt or 3YF-ShcC in mouse subcutaneous tissues

To investigate these antitransforming effects of ShcC-wt and 3YF-ShcC *in vivo*, the tumorigenicity of NB-39-nu cells expressing each mutant in nude mice was evaluated. Tumors generated by eight independent injections of each mutant were analysed in weight and histology at 4 weeks after subcutaneous injection. The results revealed a marked reduction in sizes of tumors from the cells expressing either ShcC-wt or 3YF-ShcC at this time, but not of tumors from the control cells or cells expressing ΔSH2-ShcC (Figure 7a).

The tumors from the control, ShcC-wt-expressing and ΔSH2-ShcC-expressing cells presented a hypervascular appearance (Figure 7a: upper panel), which has the histological characteristics of almost equal-sized cells with a regular arrayed pattern, high nuclear-to-cytoplasmic (N/C) ratio and chromatin-rich nucleuses (Figure 7b). On the other hand, the tumors from the 3YF-ShcC-expressing cells were hypovascular and histologically distinct from the other mutants, showing rather unequal-sized cells with an irregular arrayed pattern, a lower N/C ratio, few mitosis and decreased nucleus density. In accordance with this, staining by a proliferation marker, Ki-67, or a mitotic activity marker, cyclin A, markedly decreased in the tumors from 3YF-ShcC-expressing cells (Figure 7b), showing that the cell cycle progression was significantly suppressed by 3YF-ShcC *in vivo*, compared with the analysis by [^{3}H]-tymidine incorporation *in vitro* (Figure 2b). TUNEL staining showed no marked difference in cell apoptosis among each tumor tissue (data not shown). These results suggest that the antitumorigenic activity of the 3YF-ShcC-expressing cells *in vivo* accompanies the regulation of cell proliferation, which is distinct from the impairment of tumorigenicity by expression of ShcC-wt.

Discussion

In our previous report, the biological effects of constitutively activated signals of ALK-ShcC on the tumorigenesis of neuroblastoma cells remain to be investigated. Here, we demonstrated that the proliferation, survival and cell migration of these neuroblastoma cells were dependent on the signals via ShcC-Grb2 pathway, downstream of ALK. Additionally, overexpressed ShcC has a suppressive effect on the anchorage-independent growth of these cells via its SH2 domain and this regulation is closely associated with the regulation of c-Src and Fyn tyrosine kinases.

The fact that 3YF-ShcC significantly suppressed the activity of both ERK1/2 and Akt, suggesting that ShcC, among signaling pathways originating from activated ALK, predominantly regulates these signals through

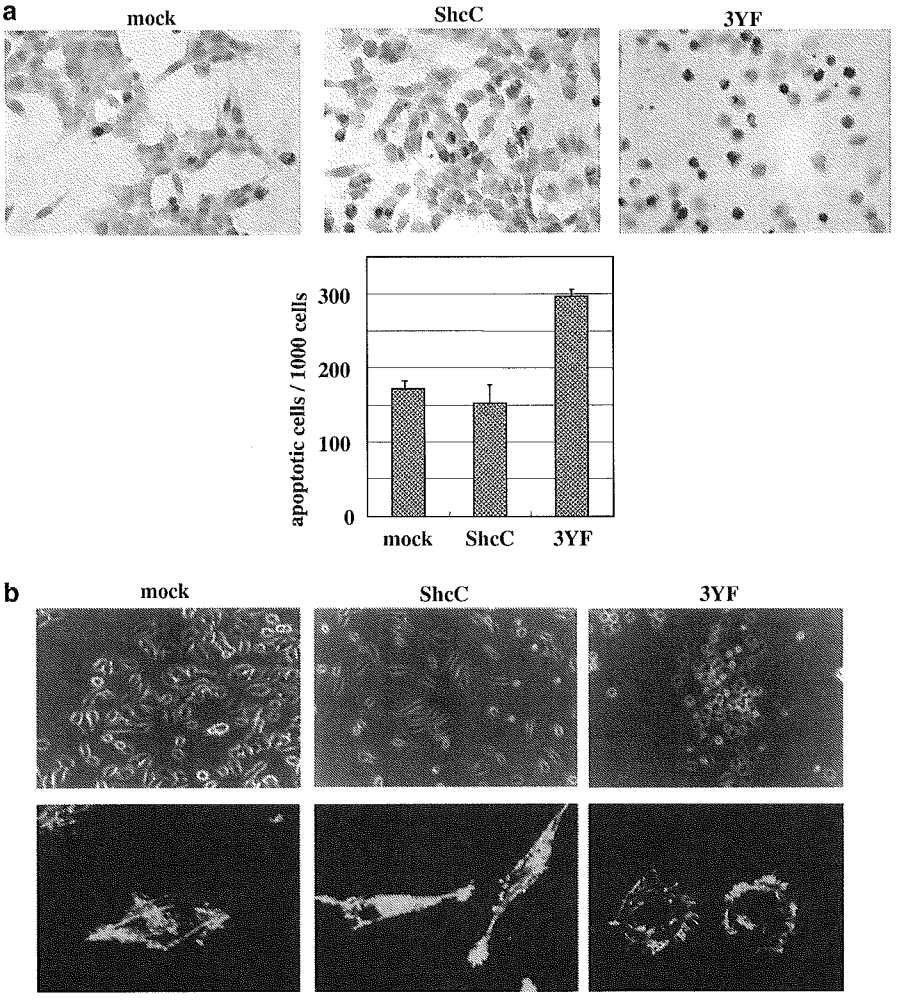

Figure 3 Effects of ShcC mutants on apoptosis and differentiation of NB-39-nu cells induced by all-*trans* retinoic acid (RA). (**a**) TUNEL analysis of ShcC mutant cells were performed as described in Materials and methods. Bar: 100 μm (upper panel). TUNEL-positive cells, the prominent dark positive cells, are counted for every 1000 cells for each slide, and three different slides were analysed for each sample. The graph represents the results (expressed as mean $\pm$ s.d.) of three observations (lower panel). (**b**) RA-induced morphological change of NB-39-nu cells expressing ShcC mutants. The cells were grown for 48 h in RPMI 1640 with 10% FCS containing 2.5 μM of RA and examined by phase-contrast microscopy (upper panel). Actin filaments stained with FITC-labeled phalloidin were visualized with a confocal fluorescence microscope (lower panel)

binding to Grb2. Our recent study also shows that the suppression of activated ALK using the RNA interference technique (RNAi) reduces the phosphorylation of ShcC, ERK1/2 and Akt, and induces the apoptotic cell death of NB-39-nu cells (Hakomori *et al.*, manuscript in preparation). The ERK and Akt pathways are key regulators of cell proliferation, survival and differentiation. Cells expressing 3YF-ShcC become more susceptible to RA-induced apoptosis presumably due to inhibition of the Akt pathway. It has recently been shown that ShcC is physiologically involved in the regulation of the PI3K/Akt pathway as a downstream effecter of the ligand-stimulated Ret receptor in neuroblastoma cells (Pelicci *et al.*, 2002). This study confirms that the survival of NB-39-nu cells is regulated by the signals downstream of ShcC. The 3YF-ShcC also causes inhibition of cell motility, while overexpressed ShcC significantly increases the ability of cell migration, indicating that ShcC positively affects the regulation of cell migration. Previously, ShcA was shown to be closely related with cell motility via the MAPK pathway (Collins *et al.*, 1999; Gu *et al.*, 1999), but the association of ShcC with the ability of cell migration has not been investigated.

The expression of 3YF-ShcC had a suppressive effect on the proliferation of NB-39-nu cells cultured *in vitro* and more significantly on the cell cycle progression of the nude mouse tumor. These data suggest that ShcC positively regulates the cell proliferation of neuronal tumor cells as well as ShcA, which has been reported to affect the tumor growth in nude mice using breast cancer cell lines (Stevenson *et al.*, 1999).

The overexpression of ShcC-wt endowed NB-39-nu cells with several characteristics. Other than the enhancement of cell migration and neurite outgrowth, which is consistent with previous study (Collins *et al.*, 1999; Pelicci *et al.*, 2002), the observation that ShcC-wt-expressing cells were impaired for anchorage-indepen-

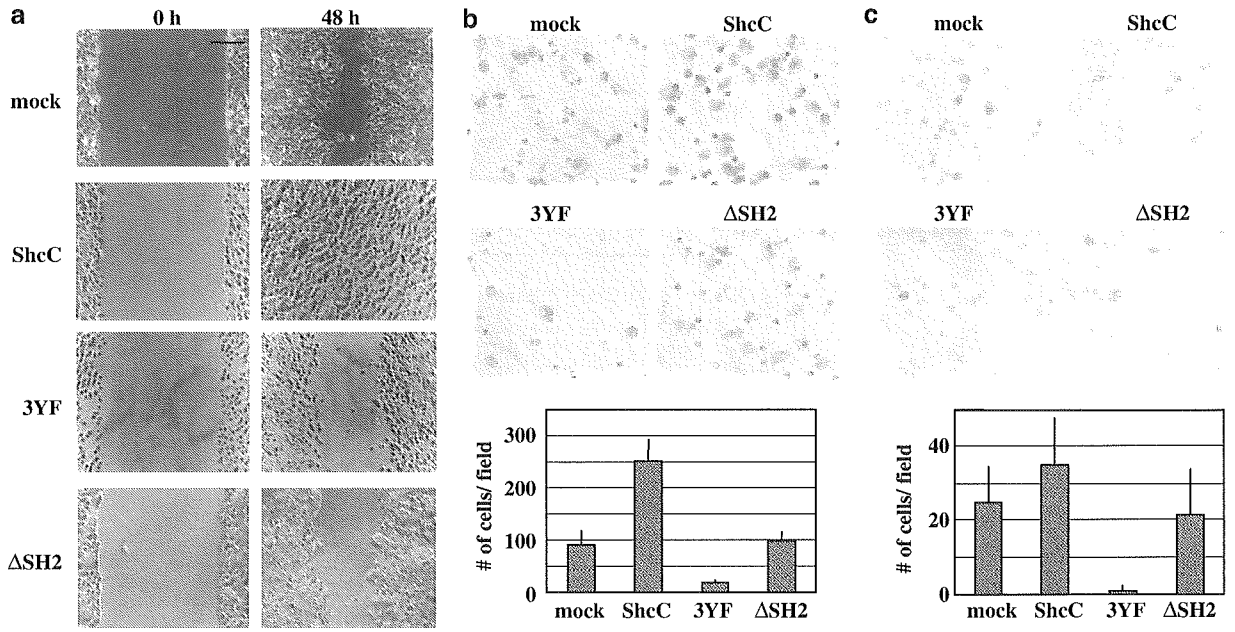

Figure 4 Expression of ShcC-wt significantly promotes the ability of cell migration in NB-39-nu cells. (**a**) Wound-healing assay for ShcC mutant cells. Photographs of the cells taken 48 h after wounding under a microscope. Bar: 200 μm. (**b**) Photographs (upper panel) and graph (lower panel) of ShcC mutant cells that have migrated through the filter by modified Boyden chamber cell migration assay. The graph represents the results (expressed as mean $\pm$s.d.) of the experiments performed in triplicate. (**c**) Photographs (upper panel) and a graph (lower panel) of the results from cell invasion assay

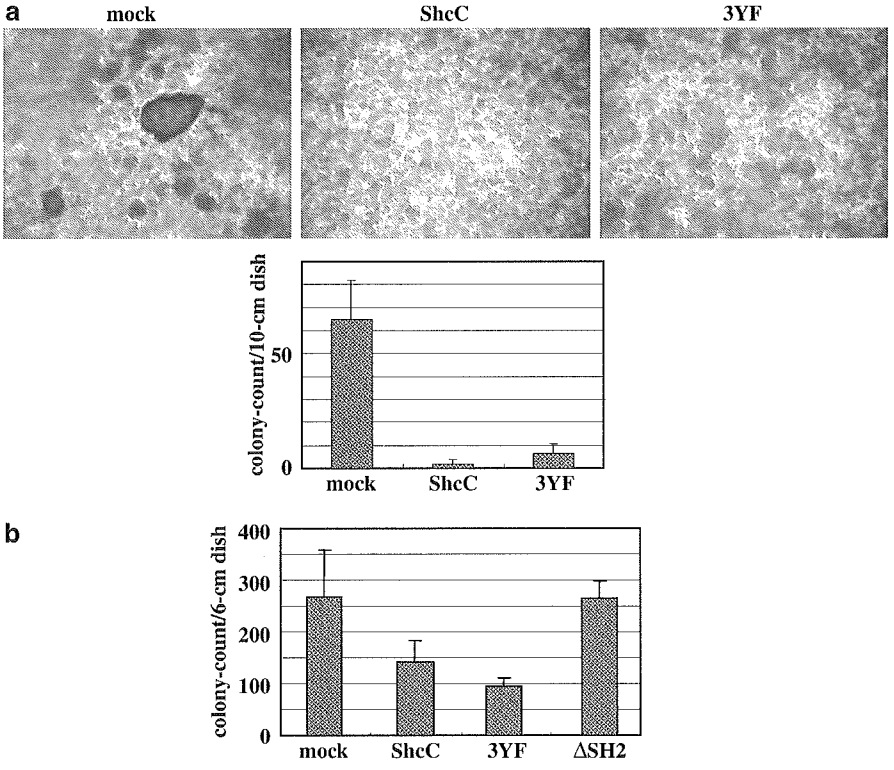

Figure 5 Evaluation of *in vitro* transforming activity in NB-39-nu cells expressing ShcC mutants. (**a**) Tendency for ShcC mutant cells to form cell aggregations on the dish surface as described in Materials and methods. Photographs of each dish were taken with a microscope at a magnification of $\times 40$ (upper panel). The graph represents the mean values ($\pm$s.d.) of three independent experiments (lower panel). (**b**) Anchorage-independent growth of ShcC mutant cells was evaluated by assaying colony formation in soft agar (performed as described in Materials and methods). The results represent the average values ($\pm$s.d.) of three replicated experiments

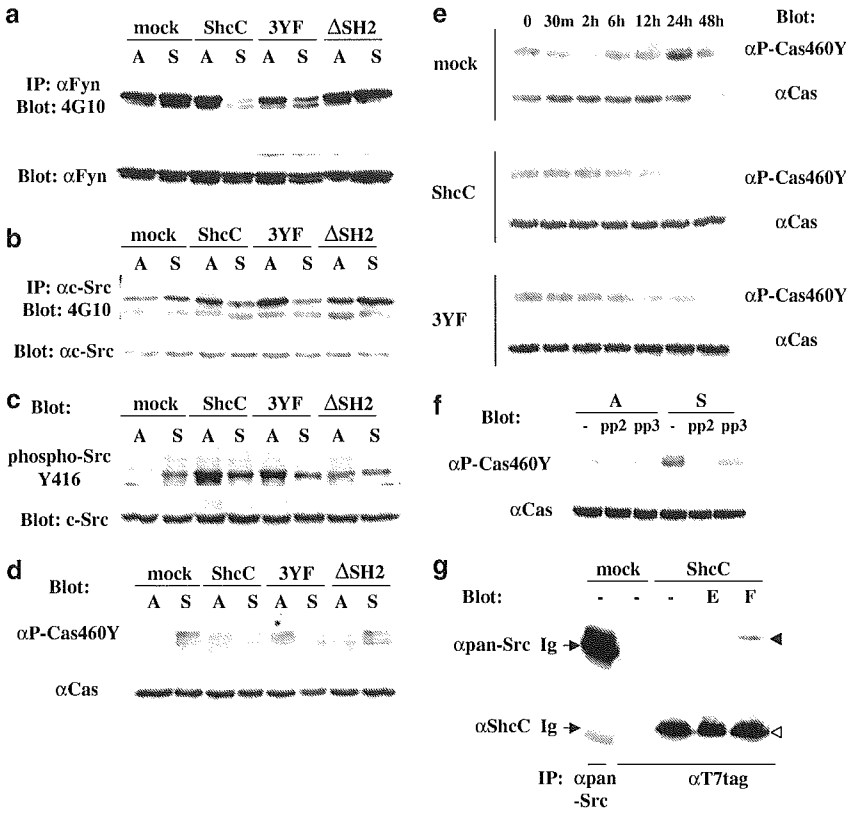

Figure 6 Anchorage-independent activation of Src family kinases (SFKs) and tyrosine phosphorylation of Cas in NB-39-nu is affected by the expression of ShcC. The cell suspension culture of ShcC mutant cells was essentially performed as described in Materials and methods. **A**: attached cells. **S**: cells in a suspended condition. Lysates were duplicated and detected by immunoprecipitation and Western analysis. (**a**, **b** and **c**) Cells cultured for 24 h in adherent or suspended conditions were analysed with the antibodies against each Src family kinase shown in the figure. Anti-phospho-Src Y416 recognizes all Src family members phosphorylated at the tyrosine corresponding to Tyr416 of avian Src. (**d**) Same analysis performed as (**a**) (**b**) and (**c**) using the antibodies against for phospho-460Y of Cas (αP-Cas460Y) and Cas protein (αCas). (**e**) Time course of tyrosine phosphorylation of Cas in each ShcC mutant cells cultured in suspension for the indicated time periods. (**f**) Effect of Src inhibitor, PP2, on the tyrosine phosphorylation of Cas in NB-39-nu control cells. The cells cultured for 24 h were harvested following treatment with 10 μM of PP2 for 2 h. As a negative control, the same dose of PP3 was used in place of PP2. (**g**) ShcC forms complex with SFKs following the stimulation of fibronectin. Lysates of mock cells and ShcC-wt cells were analysed after the stimulation with EGF or fibronectin as described in Materials and methods. -: serum free without stimulation; E: stimulated by EGF; F: stimulated by fibronectin. Ig: immunoglobulin. Anti-pan-Src antibody (SRC2) reacts with c-Src p60, Yes p62, Fyn p59, c-Fgr p55 and c-Src2. closed arrowhead: SFK; open arrowhead: p52 ShcC

dent growth and tumorigenicity suggests a novel function of ShcC. Taking into account that the expression of 3YF-ShcC but not ΔSH2-ShcC showed similar effects, the SH2 domain of ShcC may be responsible for this unique function of ShcC, distinct from ShcA. In addition, the least changes in ERK1/2 or Akt activation by overexpression of ShcC-wt suggest that this function might be independent of phosphorylation of Grb2-binding sites or the activation levels of downstream targets. There are reports showing different binding specificity towards phosphotyrosine-containing motifs among Shc families (O'Bryan *et al*., 1996a, b; Pelicci *et al*., 1996). It is crucial to identify the molecules associating with the SH2 domain of ShcC in neuroblastoma cells to elucidate the mechanism of these SH2-mediated effects of ShcC.

The smaller size of the nude mouse tumors due to the expression of ShcC-wt, regardless of mild changes in cell proliferation as both tumor tissue and culture cells, may also reflect suppression of anchorage independency (Freedman and Shin, 1974; Kumar, 1998), which results in the loss of the majority of the injected cells by anoikis before they start forming tumors. The anchorage independency of NB-39-nu mutants well corresponded to the sustained phosphorylation levels of c-Src, Fyn and Cas after cell detachment, suggesting that the expression of ShcC-wt has a negative effect on anchorage independency due to the suppression of the SFK-Cas pathway (Figure 6). It is possible that ShcC-SH2 plays a competitive role with YDYV in the Src-binding domain of Cas, judging from the consensus motifs binding to ShcC-SH2 (O'Bryan *et al*., 1996a, b), although this association was not detected by usual immunoprecipitation experiments (data not shown). On the other hand, the fact that ShcC forms the complex with SFK in this study indicates that there might be a role of association between SFK and ShcC in the regulation of tyrosine kinase activity of SFK. The fact that malignant neuroblastoma cell lines with hyperphosphorylated ShcC frequently have lower expression level

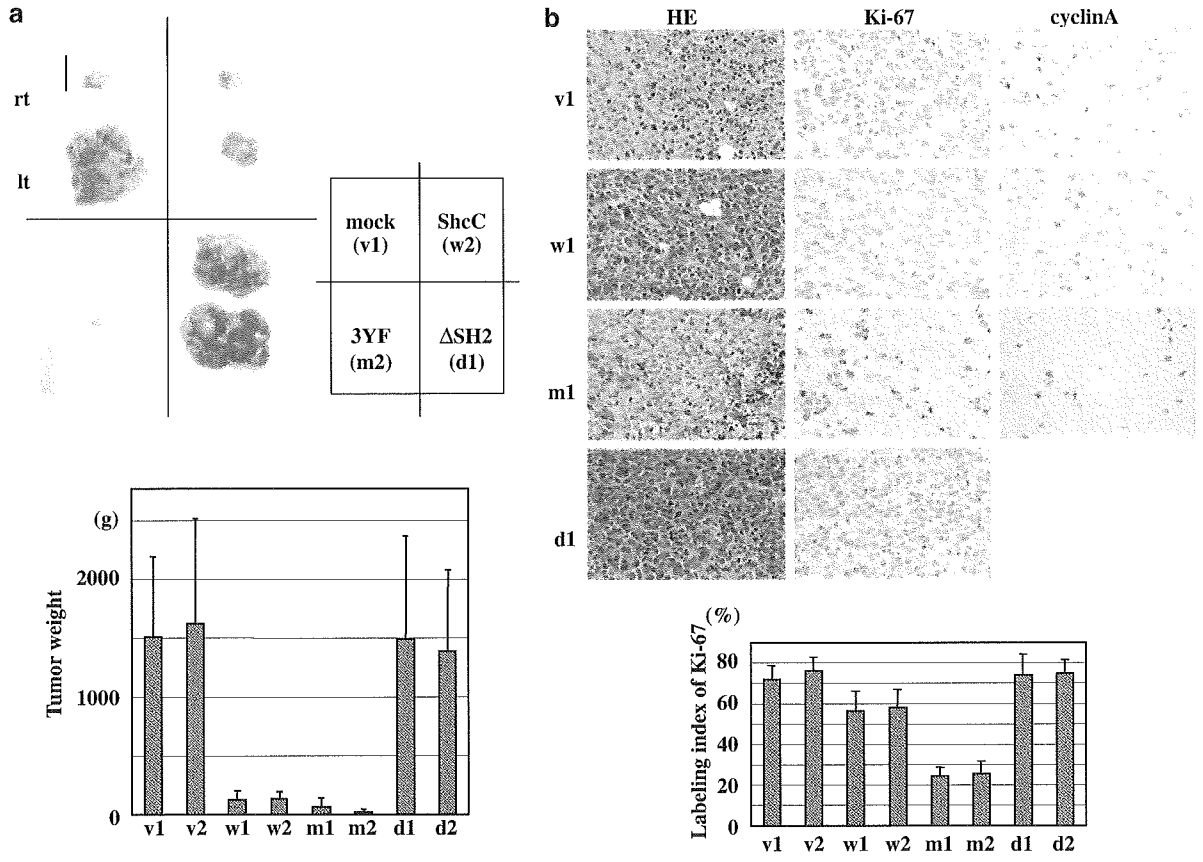

Figure 7 Nude mouse tumors derived from ShcC mutant cells. (**a**) Photographs of tumors from nude mice at three weeks after subcutaneous injection of ShcC mutant cells (upper panel). Tumorigenicity shown by the average weight (±s.d.) of the eight tumors derived from each clone (lower panel). Two independent clones are analysed for each ShcC mutant. Bar: 10 mm (**b**) Photographs of a cross-section of each tumor tissue using a microscope at a magnification of ×400. HE: tumor tissues stained with hematoxylin and eosin; Ki-67 and cyclin-A: tumor tissues immunostained against Ki-67 and cyclin-A, respectively (upper panels). The proliferating activity of each tumor was defined as the labeling index of Ki-67 by counting the positive stained cells per 1000 tumor cells. The data show the average scores±s.d. of the positive cells in three different areas of each slide (lower panel). NB-39-nu clones are described as: v1 and v2 (control), w1 and w2 (expressing ShcC-wt), m1 and m2 (expressing 3YF-ShcC), d1 and d2 (expressing ΔSH2-ShcC)

of ShcC (Miyake *et al*., 2002) might indicate additive effects of hyperphosphorylation and downregulation of ShcC on phenotype of neuroblastoma. There is the possibility that an unknown mechanism causes down-regulation of ShcC, which is hyperphosphorylated by receptor stimulation, and eventually induces malignant transition of tumors.

We have shown in this study that hyperphosphorylated ShcC in neuroblastoma cells plays an essential role in regulating cellular proliferation, survival, migration and transformation, and each domain of ShcC might differentially regulate these physiological functions. Controlling these domain-mediated signals could be a target in restricting the progression and metastasis of neuroblastoma cells.

Materials and methods

Plasmid constructions

The full-length human ShcC cDNA for transfection was donated by Dr T Nakamura (Nakamura *et al*., 1996b), and inserted into a mammalian expression vector pcDNA3.1. Tyrosine-to-phenylalanine mutations were introduced in the ShcC cDNAs by *in vitro* site-directed mutagenesis, which changed Y221/222 and Y304 to three phenylalanines (3YF-ShcC). The SH2 domain (amino acid 379–472)-deleted form of ShcC (ΔSH2-ShcC) was also generated. All parts amplified by PCR were verified by sequencing.

Cell culture, transfection

NB-39-nu cells were used in our previous report (Miyake *et al*., 2002). The stable expression of ShcC mutants, the full-length of ShcC (ShcC-wt), 3YF-ShcC and ΔSH2-ShcC in NB-39-nu cells were obtained by transfection using Fugene™ 6 transfection reagent (Roche Molecular Biochemicals) according to the manufacturer's instructions. Then, cell clones were obtained from individual G418-resistent colonies and subjected to Western blot screening using the T7 tag antibody (Novagen). These cells were cultured in an RPMI 1640 medium with 10% FCS (Sigma) at 37°C in 5% CO_2. A suspension culture of the cells was essentially performed according to a previously published procedure (Folkman and Moscona, 1978; Frisch and Francis, 1994; Wang and Sheibani, 2002). In this study, LOW-CELL-BINDING 90 mm-Petri dishes treated with 2-Methacryloxyethyl Phosphorylcholine (MPC) (Nalge Nunc International) were used instead of poly-HEMA-coated dishes.

The cells were grown to confluence in tissue culture dishes, and were then trypsinized and plated at a concentration of 1×10^6 cells/90 mm dish into MPC-treated Petri dishes and cultured for 0–48 h. The cells were then collected by pipetting, washed by PBS and extracted with PLC-lysis buffer (Rozakis-Adcock *et al*., 1993) for the Western analysis.

Preparation of specific antibodies, cell stimulation, immunoprecipitation and immunoblotting

The polyclonal antibodies against the CH1 domains of ShcC (amino acid 306–371) and against Cas protein (αCas) were prepared as described (Sakai *et al*., 1994, 2000). A phospho specific polyclonal antibody against Cas (αP-Cas460Y) was generated by immunizing rabbits with a synthetic peptide, CAEDV(pY)DVP, which is a representative of the repetitive tyrosine-containing motifs in the substrate domain of Cas, after being conjugated with thyroglobulin. Other antibodies were purchased as follows: anti-phosphotyrosine antibody (4G10) (Upstate Biotechnology, Inc), anti-p44/42 MAPK (ERK1/2) and anti-phospho-p44/42 MAPK (phospho-ERK1/2) antibodies (BioLabs), anti-Akt and anti-phospho-Akt (Ser473) antibodies (Cell Signaling), anti-c-Src antibody (Upstate Biotechnology, Inc.), anti-phospho Src family (Tyr416) antibody (Cell Signaling), anti-Fyn antibody and anti-pan-Src antibody (SRC2) (SantaCruz Biotechnology, Inc.). As secondary antibodies, horseradish peroxidase (HRP)-conjugated anti-rabbit and anti-mouse Ig (Amersham) were used. Cell-stimulation analysis with epidermal growth factor (EGF; Wako) was performed as described. The cells were starved for 24 h and treated for 5 min with EGF (100 ng/ml) (Miyake *et al*., 2002). As for stimulation with fibronectin, cultured cells were starved for 24 h then trypsinized without FCS and after the suspending condition for 30 min, seeded onto fibronectin (10 μg/ml)-coated dishes and harvested after 1 h using PLC lysis buffer. Control cells were harvested before the attachment on the fibronectin-coated surface. The immunoprecipitation and Western analysis were performed using the procedure described in the previous report (Miyake *et al*., 2002).

Evaluation of tendency to form cell aggregations on dish surface

Cells were seeded onto plastic dishes (1×10^6 cells per 100-mm diameter dish). After 5 days, distinctive colonies of cell aggregations proliferated independently of the attachment to the dish surface, and each of them consisted of more than 10 cells per dish. The data were obtained from three independent experiments.

Soft agar colony-formation assay

Anchorage-independent growth was determined by assaying colony formation in soft agar as described in the previous report (Honda *et al*., 1998). Briefly, 10^5 trypsinized cells were resuspended in DMEM containing 10% FCS and 0.4% Sea Plaque GTG agarose (Bioproduct) and poured onto bottom agar containing 10% FCS and 0.53% agarose in 6-cm culture dishes. The cells were then incubated at 37°C with 5% CO_2. After 14 days, colonies containing more than five cells were counted under the microscope.

Wound-healing assay

A wound-healing assay was performed according to the method used previously (Honda *et al*., 1999). Briefly, cells were grown to confluence in Matrigel-coated plastic culture dishes, and a wound was made using a sterile micropipette tip. Cell movement was assessed 24 and 48 h after wounding under the microscope at a magnification of × 100.

Cell migration and invasion assay

Cell invasion was analysed according to the procedure of the Boyden chamber cell migration assay with some modification (Honda *et al*., 1999), using a FALCON™ Cell Culture Insert, a chamber with a pore size of 8 μm (Becton Dickinson Labware) whose interior was filled with a plug of 10 μg Matrigel (IWAKI) per filter. A total of 1×10^5 cells in 200 μl of serum-free medium were plated in the Matrigel chamber, and a serum-free medium containing 50 μg/ml of fibronectin was placed in the 24-well plate as a lower chamber, then incubated for 12 h at 37°C in 5% CO_2. The number of cells migrated through the Matrigel to the underside of the filter was counted under the microscope. The same procedure was performed without Matrigel coating for the analysis of cell migration.

*Apoptosis of neuroblastoma cells induced by all-*trans *RA*

Cells, were seeded into 24-well tissue culture plates at a density of 5×10^4 cm^{-2} and cultured in the presence of the indicated concentration of RA (all-*trans* form; Sigma) dissolved in 70% ethanol. Control cultures were treated with the same concentration of ethanol. To identify RA-induced apoptotic reaction, TUNEL (TdT-mediated dUTP-biotin nick end labeling) was performed according to the manufacturer's instructions (In Situ Cell Death Detection, POD: Roche) as described by Gavrieli *et al*. (1992). The cells were counterstained with hematoxylin-eosin.

[^{3}H]thymidyne incorporation assay

This was performed essentially as described previously (McNeil *et al*., 1985). A total of 2×10^4 cells were seeded onto 24-well dishes and cultured for 48 h and shifted to a serum-free medium, and then 24 h later were followed by overnight stimulation with 100 ng/ml EGF. [^{3}H]thymidine (1 μCi/ml) was added for the last 4 h of incubation. The amount of incorporated [^{3}H]thymidine radioactivity was measured by liquid scintillation counting. Results are expressed as disintegrations per minute of incorporated [^{3}H]thymidine per well.

Generation of tissue samples and histological evaluation

Nude mouse tumors were obtained by independent injections of 5×10^6 ShcC mutant cells into the bilateral subcutaneous tissues of each mouse. Tumor tissues were fixed in formalin at 4°C, transferred to 70% ethanol, and blocked in paraffin. Sections were stained with hematoxylin and eosin.

Immunohistochemistry

The sections of the tumor tissues from ShcC mutant cells were immunostained with anti-Ki-67 antibody (DAKO) and anti-cyclin-A antibody (Novocastra Laboratories) using the labeled streptavidin biotin (LSAB) methods according to the manufacturer's instructions of the LSAB kit (Dako). All the primary antigens were used at a 1 : 100 dilution. Peroxidase activity was visualized with 3, 3′-diaminobebenzidine (DAB).

Acknowledgements
This study was supported by the Program for Promotion of Fundamental Studies in Health Sciences of Organization for Pharmaceutical Safety and Research of Japan, and was also supported by a grant from SBS, Inc. Izumi Miyake is the recipient of Research Resident Fellowships from the Japan Health Sciences Foundation.

References

Andrechek ER, Hardy WR, Siegel PM, Rudnicki MA, Cardiff RD and Muller WJ. (2000). *Proc. Natl. Acad. Sci. USA*, **97,** 3444–3449.

Collins LR, Ricketts WA, Yeh L and Cheresh D. (1999). *J. Cell Biol.*, **147,** 1561–1568.

Folkman J and Moscona A. (1978). *Nature*, **273,** 345–349.

Freedman VH and Shin SI. (1974). *Cell*, **3,** 355–359.

Frisch SM and Francis H. (1994). *J. Cell Biol.*, **124,** 619–626.

Gavrieli Y, Sherman Y and Ben-Sasson SA. (1992). *J. Cell Biol.*, **119,** 493–501.

Giancotti FG. (1997). *Curr. Opin. Cell. Biol.*, **9,** 691–700.

Gu J, Tamura M, Pankov R, Danen EH, Takino T, Matsumoto K and Yamada KM. (1999). *J. Cell Biol.*, **146,** 389–403.

Honda H, Nakamoto T, Sakai R and Hirai H. (1999). *Biochem. Biophys. Res. Commun.*, **262,** 25–30.

Honda H, Oda H, Nakamoto T, Honda Z, Sakai R, Suzuki T, Saito T, Nakamura K, Nakao K, Ishikawa T, Katsuki M, Yazaki Y and Hirai H. (1998). *Nat. Genet.*, **19,** 361–365.

Iwahara T, Fujimoto J, Wen D, Cupples R, Bucay N, Arakawa T, Mori S, Ratzkin B and Yamamoto T. (1997). *Oncogene*, **14,** 439–449.

Kumar CC. (1998). *Oncogene*, **17,** 1365–1373.

McNeil PL, McKenna MP and Taylor DL. (1985). *J. Cell Biol.*, **101,** 372–379.

Miyake I, Hakomori Y, Shinohara A, Gamou T, Saito M, Iwamatsu A and Sakai R. (2002). *Oncogene*, **21,** 5823–5834.

Morris SW, Naeve C, Mathew P, James PL, Kirstein MN, Cui X and Witte DP. (1997). *Oncogene*, **14,** 2175–2188.

Nakamura N, Chin H, Miyasaka N and Miura O. (1996a). *J. Biol. Chem.*, **271,** 19483–19488.

Nakamura T, Sanokawa R, Sasaki Y, Ayusawa D, Oishi M and Mori N. (1996b). *Oncogene*, **13,** 1111–1121.

O'Bryan JP, Martin CB, Songyang Z, Cantley LC and Der CJ. (1996a). *J. Biol. Chem.*, **271,** 11787–11791.

O'Bryan JP, Songyang Z, Cantley L, Der CJ and Pawson T. (1996b). *Proc. Natl. Acad. Sci. USA*, **93,** 2729–2734.

Parsons JT and Weber MJ. (1989). *Curr. Top. Microbiol. Immunol.*, **147,** 79–127.

Pawson T, Gish GD and Nash P. (2001). *Trends Cell Biol.*, **11,** 504–511.

Pelicci G, Dente L, De Giuseppe A, Verducci-Galletti B, Giuli S, Mele S, Vetriani C, Giorgio M, Pandolfi PP, Cesareni G and Pelicci PG. (1996). *Oncogene*, **13,** 633–641.

Pelicci G, Lanfrancone L, Grignani F, McGlade J, Cavallo F, Forni G, Nicoletti I, Pawson T and Pelicci PG. (1992). *Cell*, **70,** 93–104.

Pelicci G, Troglio F, Bodini A, Melillo RM, Pettirossi V, Coda L, De Giuseppe A, Santoro M and Pelicci PG. (2002). *Mol. Cell. Biol.*, **22,** 7351–7363.

Rozakis-Adcock M, Fernley R, Wade J, Pawson T and Bowtell D. (1993). *Nature*, **363,** 83–85.

Sakai R, Henderson JT, O'Bryan JP, Elia AJ, Saxton TM and Pawson T. (2000). *Neuron*, **28,** 819–833.

Sakai R, Iwamatsu A, Hirano N, Ogawa S, Tanaka T, Mano H, Yazaki Y and Hirai H. (1994). *EMBO J.*, **13,** 3748–3756.

Sidell N, Altman A, Haussler MR and Seeger RC. (1983). *Exp. Cell Res.*, **148,** 21–30.

Stevenson LE, Ravichandran KS and Frackelton Jr AR. (1999). *Cell Growth Differ.*, **10,** 61–71.

Thomas D and Bradshaw RA. (1997). *J. Biol. Chem.*, **272,** 22293–22299.

van der Geer P, Wiley S, Gish GD and Pawson T. (1996). *Curr. Biol.*, **6,** 1435–1444.

van der Geer P, Wiley S, Lai VK, Olivier JP, Gish GD, Stephens R, Kaplan D, Shoelson S and Pawson T. (1995). *Curr. Biol.*, **5,** 404–412.

Wang Y and Sheibani N. (2002). *J. Cell. Biochem.*, **87,** 424–438.

Wary KK, Mainiero F, Isakoff SJ, Marcantonio EE and Giancotti FG. (1996). *Cell*, **87,** 733–743.

Wary KK, Mariotti A, Zurzolo C and Giancotti FG. (1998). *Cell*, **94,** 625–634.

Wei L, Yang Y, Zhang X and Yu Q. (2002). *J. Cell. Biochem.*, **87,** 439–449.

Weng Z, Thomas SM, Rickles RJ, Taylor JA, Brauer AW, Seidel-Dugan C, Michael WM, Dreyfuss G and Brugge JS. (1994). *Mol. Cell. Biol.*, **14,** 4509–4521.

Windham TC, Parikh NU, Siwak DR, Summy JM, McConkey DJ, Kraker AJ and Gallick GE. (2002). *Oncogene*, **21,** 7797–7807.

Supplementary Information accompanies the paper on Oncogene website (http://www.nature.com/onc)

American Journal of Pathology, Vol. 167, No. 1, July 2005

Tumorigenesis and Neoplastic Progression

Biological Role of Anaplastic Lymphoma Kinase in Neuroblastoma

Yuko Osajima-Hakomori,*¶‖ Izumi Miyake,*† Miki Ohira,‡ Akira Nakagawara,‡ Atsuko Nakagawa,§ and Ryuichi Sakai*

From the Growth Factor Division, National Cancer Center Research Institute, Chuo-ku, Tokyo; St. Marianna University School of Medicine,¶ Kawasaki-shi, Kanagawa; Tokyo Metropolitan Geriatric Hospital,‖ Itabashi-ku, Tokyo; the Department of Pediatrics,† Kitasato University School of Medicine, Sagamihara-shi, Kanagawa; the Division of Biochemistry,‡ Chiba Cancer Center Research Institute, Cyuo-ku, Chiba; and the Department of Pathology,§ Aichi Medical University, Aichi-gun, Aichi, Japan*

Anaplastic lymphoma kinase (ALK) is a tyrosine kinase receptor originally identified as part of the chimeric nucleophosmin-ALK protein in the t(2;5) chromosomal rearrangement associated with anaplastic large cell lymphoma. We recently demonstrated that the ALK kinase is constitutively activated by gene amplification at the ALK locus in several neuroblastoma cell lines. Forming a stable complex with hyperphosphorylated ShcC, activated ALK modifies the responsiveness of the mitogen-activated protein kinase pathway to growth factors. In the present study, the biological role of activated ALK was examined by suppressing the expression of ALK kinase in neuroblastoma cell lines using an RNA interference technique. The suppression of activated ALK in neuroblastoma cells by RNA interference significantly reduced the phosphorylation of ShcC, mitogen-activated protein kinases, and Akt, inducing rapid apoptosis in the cells. By immunohistochemical analysis, the cytoplasmic expression of ALK was detected in most of the samples of neuroblastoma tissues regardless of the stage of the tumor, whereas significant amplification of ALK was observed in only 1 of 85 cases of human neuroblastoma samples. These data demonstrate the limited frequency of ALK activation in the real progression of neuroblastoma. *(Am J Pathol 2005, 167:213–222)*

Receptor tyrosine kinases (RTKs) play an important role in regulating diverse cellular processes, such as proliferation, differentiation, survival, motility, and malignant transformation. The activation of RTKs typically requires ligand-induced receptor oligomerization, which results in tyrosine autophosphorylation of the receptors at tyrosine residues.[1–3] By recruiting specific sets of signal transducer molecules in a phosphorylation-dependent manner, each RTK is capable of inducing individual, specific cellular responses.[4] On the other hand, activation of RTKs by either mutations or overexpression is frequently found in various human malignancies.[3,5]

Anaplastic lymphoma kinase (ALK) is a 200-kd tyrosine kinase encoded by the *ALK* gene on chromosome 2p23. ALK was first identified as part of an oncogenic fusion tyrosine kinase, nucleophosmin-ALK, which is associated with anaplastic large cell lymphoma.[6,7] It was also found as a form of fusion protein with a clathrin heavy chain (CTCL) in myofibroblastic tumors.[8] Full-length ALK has the typical structure of an RTK, with a large extracellular domain, a lipophilic transmembrane segment, and a cytoplasmic tyrosine kinase domain.[9,10] ALK is highly homologous to leukocyte tyrosine kinase (LTK) and is further classified into the insulin receptor superfamily. The *LTK* gene is mainly expressed in pre-B lymphocytes and neuronal tissues,[11–13] whereas expression of the normal *ALK* gene in hematopoietic tissues has not been detected. Instead, it is dominantly expressed in the neural system.[14,15] In the developing brains of mice, specific expression of *ALK* was seen in the thalamus, mid-brain, olfactory bulb, and selected cranial regions, as well as the dorsal root, the ganglia of mice,[9,10,16] suggesting a specific role in the development of the embryonic nervous system. Currently, however, the function of ALK in adult normal tissue or carcinogenesis remains an open question. Several studies have recently indicated pleiotrophin or midkine as possible ligands for ALK.[17,18] Although they appeared to induce the functional activa-

Supported by the Program for the Promotion of Fundamental Studies in Health Science of the Organization for Pharmaceutical Safety and Research of Japan. Y.O-H. is the recipient of a Research Resident Fellowship from the Foundation for Promotion of Cancer Research, Japan.

Accepted for publication March 23, 2005.

Address reprint requests to Ryuichi Sakai, M.D., Growth Factor Division, National Cancer Center Research Institute, 5-1-1 Tsukiji, Chuo-ku, Tokyo 104-0045, Japan. E-mail: rsakai@gan2.res.ncc.go.jp.

tion of ALK, it is still unclear whether these molecules are the physiological ligands of ALK.

Neuroblastoma is one of the most common pediatric tumors derived from the sympathoadrenal linage of the neural crest. Tumors found in patients under the age of 1 year are usually favorable and often show spontaneous differentiation and regression.[19] Amplification of the N-*myc* gene occurs in approximately 25% of neuroblastomas and correlates with the aggressiveness of the disease. In addition to N-*myc* gene amplification, the expression of various genes has significant correlation with the stage of and prognosis for neuroblastoma. A high level of TrkA expression is predictive of a favorable outcome,[20] whereas TrkB is highly expressed in immature neuroblastomas with N-*myc* amplification.[21] High expression of caspase-1, -3, and -8 is correlated with favorable neuroblastomas.[22,23] On the other hand, survivin, which suppresses caspase and promotes the cell survival signal, is significantly expressed,[24] and telomerase is activated[25] in unfavorable tumors. There may be a critical difference in the expression of other molecules, including RTKs, in neuroblastoma. A recent paper showed that full-length ALK is detected in almost one-half of the cell lines derived from neuroblastomas and neuroectodermal tumors.[26] We have recently shown using mass-spectrometry analysis that ALK is a major phosphoprotein associated with hyperphosphorylated ShcC in several neuroblastoma cell lines.[27] In these cells, ALK was markedly activated, and it induced the constitutive phosphorylation of ShcC and mitogen-activated protein kinase (MAPK), regardless of stimulation by epidermal growth factor (EGF) or nerve growth factor.[27] These findings strongly suggest that constitutively activated ALK kinase plays a physiological role in the development of neuroblastoma.

In this study, we investigated the biological function of the constitutively activated ALK kinase in neuroblastoma. The RNA interference (RNAi) technique using specific sets of small interfering RNA (siRNA) was induced to inhibit the *ALK* gene expression in human neuroblastoma cells with or without gene amplification of *ALK*. The effects of disrupted ALK expression on cell survival or downstream signaling, such as MAPKs or Akt pathways, are examined to understand the biological meaning of ALK amplification in neuroblastoma cells. We also performed Southern blot analysis of primary neuroblastoma tumors from 85 patients to check whether the *ALK* gene amplification was actually present in neuroblastoma tissues. Furthermore, we sought the *ALK* gene expression in human neuroblastoma tissues using immunohistochemical analysis.

Materials and Methods

Cell Culture

Cell lines of human neuroblastoma were maintained in RPMI 1640 supplemented with 10% fetal calf serum (Sigma, St. Louis, MO), penicillin, and streptomycin at 37°C in a humidified 5% CO_2 incubator.

Reverse Transcription-Polymerase Chain Reaction (RT-PCR) Analysis

Total RNA was extracted with ISOGEN (Nippongene Japan, Toyama, Japan) from NB-39-nu and SK-N-MC cells. The PCR primer pair 5′-AGGTTCTGGCTGCAGATGGT-3′ and 5′-ACATTGTTCTCTCGAGTGCAGAC-3′ corresponding to the cytoplasmic portion of human ALK was prepared. As much as 0.25 μg of total RNA was reverse transcribed and amplified with the SuperScript One-step RT-PCR with the Platinum *Taq* kit (Invitrogen Life Technologies, Carlsbad, CA) in a total volume of 50l including 2× reaction mix, 0.2 μmol/L of each primer, and 1 μl of RT/Platinum *Taq* Mix. Amplification conditions consisted of cDNA synthesis and predenaturation at 50°C for 30 minutes and 94°C for 2 minutes followed by 25 cycles at 94°C for 15 seconds, 58°C for 30 seconds, and 72°C for 45 seconds. A final amplification for 7 minutes at 72°C finished the PCR. The product was separated with 1.2% agarose gel electrophoresis and analyzed using the Quality One System (Bio-Rad, Hercules, CA).

Immunochemical Analysis of Proteins

Immunoprecipitation and immunoblotting were performed as described previously.[27] The polyclonal antibodies against the CH1 domains of ShcC (amino acids 306–371) and the anti-ALK antibody (αALK) that was against the cytoplasmic portion (amino acid 1379–1524) of human ALK were prepared as described previously.[27,28] An anti-phosphotyrosine antibody (4G10) was obtained from UBI. Anti-p44/42 MAPKs, anti-phospho-p44/42 MAPKs, anti-Akt, and anti-phospho-Akt antibodies were purchased from Cell Signaling (Beverly, MA). Anti-EGF receptor (EGFR), anti-Ret, and anti-TrkA antibodies were purchased from Santa Cruz Biotechnology (Santa Cruz, CA). *In vitro* kinase assay for ALK was performed as previously described.[27] Anti-ALK immunoprecipitates were incubated with or without Poly-Glu/Tyr as an exogenous substrate.

Immunocytostaining

For ALK/TOTO-3, immunostaining using anti-ALK antibody was performed at first, and then nuclei were stained using TOTO-3. The cells seeded on the 24-well plates were washed with phosphate-buffered saline (PBS) three times and fixed with 4% paraformaldehyde (methanol free) for 5 minutes at room temperature. The cells were rinsed with PBS twice and then permeabilized with 0.2% Triton X-100 solution in PBS for 10 minutes at room temperature. The cells were blocked with 5% goat serum and 3% bovine serum albumin–Tris-buffered saline for 30 minutes at room temperature. The blocking solution was drained off, and the cells were incubated with a 1:1000 dilution of αALK for 1 hour at room temperature. The cells were rinsed with PBS three times and incubated with a 1:2000 dilution of Alexa fluor (Molecular Probes, Eugene, OR) and 1: 100 dilution of TOTO-3 (Molecular Probes) for